NASA TT F-10,248

DAMPING OF VIBRATIONS OF THE BLADING OF AN OPERATING TURBINE

J. L. Deschamps

Translation of "Sur l'amortissement des vibrations d'un aubage de turbomachine en fonctionnement"
Publications Scientifiques et Techniques du Ministère de l'Air, No. 421, Paris, 1965

NATIONAL AERONAUTICS AND SPACE ADMINISTRATION
WASHINGTON SEPTEMBER 1966

CONTENTS

DAMPING OF VIBRATIONS OF THE BLADING OF AN OPERATING TURBINE

J. L. Deschamps

ABSTRACT

An attempt to provide a rational explanation of some results obtained from wind-tunnel experiments on turbine blading. A distribution of aerodynamic singularities, characteristic of the stability of a viscous flow, supplies the aerodynamic forces in a system of blading, starting from the velocity diagram. The method of concentrated masses makes it possible to express the mechanical forces developed during vibration. The transient aerodynamic regime features a cyclical deformation of the velocity diagram, which modifies the expression for the circulation in the steady-state regime. With the alternate detachments and reattachments at the profile points, a supplementary term appears which can, in agreement with certain experimental results, change the sign of the damping coefficient.

Synopsis

This paper may not appear to have any particularly remarkable scientific character for the informed reader. It did result as a plausible explanation of some wind-tunnel experiments for which no satisfactory interpretation was found immediately. Other work will certainly have to be carried out to establish the relation between this result and certain surprising experiences which industry has encountered occasionally on the subject of vibrations in turbines. However, it may still be of interest to attempt such a synthesis in regard to a problem which is generally treated in its separate elements.

The six chapters of this study are organized as follows:

Chapter 1 expounds the essential principles and gives a conclusion;

Chapter 2 describes the mathematical model selected to symbolize the flow of fluid in axial-flow turbines;

Chapter 3 is an analysis of the forces generated within the blading of a turbine;

Chapter 4 contains an approach to the solution of the equations stated in the preceding chapters;

Chapter 5 outlines, from the general solutions obtained, the mathematical form of the damping where the parameters are the state of the gas, the geometry of the blading, and time;

Chapter 6 is the numerical application to a particular case actually experimented and specifies to what extent the proposed theory represents the observed phenomena.

NOTATIONS

(Given in order of appearance in text)

Φ	Theoretical potential function representing flow in blading developed along the plane xOy (fig. 1).
γ	Curl of the velocity vector around a blade profile.
z	Complex affix X-iY (fig. 2).
τ	Developed blade pitch or distance between two consecutive vortices.
$\overline{W_1}$	Relative velocity at blade intake.
$\overline{W_2}$	Relative velocity at blade discharge.
$\overline{W_m}$	(geometric) mean $\frac{\overline{W_1} + \overline{W_2}}{2}$.
α	$(\overline{W_m}, Oy)$ angle (figs. 4, 5, 6).
n	Order number of a vortex counted positively from Oy (fig. 2).
$2N + 1$	Number of developed blades.
Φ_0	Potential function representing flow generated by an isolated vortex.
W_{x_0}	Component along Ox of aerodynamic velocity deduced from Φ_0.
W_{y_0}	Component along Oy of aerodynamic velocity deduced from Φ_0.
r	Polar radius in XOY coordinates.
θ	Polar azimuth in XOY coordinates.
Φ_s	Approximate potential function representing flow in the developed blading.
Z	Function of z defined by the equation

$$Z = \frac{\pi z}{\tau \cdot e^{i\alpha}}.$$

λ Vectorial modulus defined by equation

$$\lambda = \frac{\pi r}{\tau}.$$

h_0 Scalar defined by the relation

$$h_0 = e^{-2\lambda \sin(\theta - \alpha)}.$$

a_0 Scalar defined by the relation

$$a_0 = \cos \{ 2\lambda \cdot \cos(\theta - \alpha) \}.$$

b_0 Scalar defined by the relation

$$b_0 = \sin \{ 2\lambda \cdot \cos(\theta - \alpha) \}.$$

W_x Component along OX of aerodynamic velocity deduced from Φ_s.

W_y Component along OY of aerodynamic velocity deduced from Φ_s.

i_t Inclination of absolute velocity at intake along axis of turbine.

m Inclination of relative velocity W_1 (theoretically at infinity upstream) along axis of turbine.

V_1 Absolute aerodynamic velocity at intake (theoretically at infinity upstream).

ψ Deviation of flow due to blades.

A Angle defined by one of the relations

$$A = \arccos a_0 = \arcsin b_0.$$

q Flow volume of fluid in blading channel constituted by two consecutive blades.

m_s Specific weight of fluid.

l Height of blade (distance along Ox between bottom and top of blade).

$\overline{F}$ Aerodynamic force applied to blade.

$\overline{F_y}$ Component of $\overline{F}$ along Oy.

$\overline{F_u}$ Component of $\overline{F}$ along Ou.

e Width of rotor taken parallel tc Ou axis.

ω Frequency of blade vibration.

y_p Pseudo-amplitude of real blade vibration (assumed to vary slowly in time).

t_d Mean duration of stay of fluid molecule in blading.

a_d Distance from point of detachment to tip of profile.

e_p Angular spread between W_2 and the tangent to the exterior blade curve.

c_d Chord of blade profile at profile tip.

Re Reynolds number defined by $\mathbf{Re} = \frac{W_m c_d}{\nu}$ if Re is independent of τ, or by $\mathbf{Re} = \frac{W_m D_h}{\nu}$ if Re depends on τ.

D_h Hydraulic diameter defined by

$$D_h = \frac{4 \tau \cos \theta_1 \cdot l}{2 (l + \tau \cos \theta_1)}.$$

ν Kinematic viscosity.

$d_p(\mathrm{Re})$ Function of Reynolds number Re.

j Phaseshift between blade oscillation and excitation by the fluid (negative and greater than -90^o).

E Elastic modulus of metal utilized for blades.

I Moment of inertia of the straight section of the blade (assumed as constant).

$y(x, t)$ Function of x and of time t obtained from the product of a function of x, f(x) and of a function of t, h(t).

$f(x)$ Function of x defining the form of the elastic line at a given instant t.

$h(t)$ Function of time defining oscillation of a point of the elastic line of abscissa x.

K Constant introduced by separation of the variables x and t according to f(x) and h(t).

R Radius along which blades are mounted (blade bottom).

q' Order number of the concentrated mass of the total blade mass at several points of the elastic line where the number $2n' + 1$ may increase as a function of the degree of precision desired in the evaluation of the elastic forces.

n' Whole number whose definition results from that of q'.

ω_r Frequency of the rotation of turbine.

N_m Rate of rotation of turbine in revolutions per second.

U Intermediate grouping defined by

$$U = \sqrt{\frac{P \cdot \omega_r^2 \cdot R}{EI}}.$$

k Constant related to K by

$$k^2 = \frac{K \cdot l}{2I\left(\frac{l}{2}\right)}.$$

P Weight of blade.

M Mach number.

$\mathcal{M}_0$ Aerodynamic moment in the axes yOx.

F_{y_0} Component of F_y independent of time.

F_{y_1} Component of F_y which is a function of time.

γ_0 Component of γ independent of time.

γ_1 Amplitude of the alternate component of γ.

V_n Angle formed by the vector radius v_n and the tangent at the point of order n.

B_n Angle formed by the vector radius v_a and the tangent at the point of order n - 1.

N_p Natural frequency of each cascade blade in the absence of aerodynamic forces.

a Coefficient of the term for vibratory inertia.

b Coefficient of the term for vibratory damping.

c Coefficient of the term for vibratory elongation.

d Constant term of the vibratory equation.

I_e Coefficient of interaction (or influence) between the vibratory amplitudes of two adjacent blades.

f Coefficient of the term for self-excitation of the fluid.

N_0 Number of blades; according to a preceding notation,

$$N_0 = 2N + 1.$$

ω_0 Natural frequency of each cascade blade in the absence of aerodynamic forces.

ω_e Stray-excitation frequency.

b_1 Component of b which is a function of the incident relative velocity.

b_2 Component of b which is independent of the incident relative velocity.

d_0 Characteristic damping of the material.

A_m Apparent damping in the absence of detachment.

T_1, T_2 Coefficients of integration.

y_M Maximum relative to y at instant t.

e_f Angle formed by the tangent to the profile and the tangent to the frame at the profile tip.

N_b Pressure number.

W_{x_c} In contrast to W_x, this designates a reference velocity in the calculations of Chapter 6.

i Notation adopted by the researchers to designate ψ.

α_2 Designates, in Chapter 6, the angle formed with the axis or by the relative velocity at the blade discharge (notation derived from experimentation).

α_1 Notation adopted by the researchers to designate m.

α_v True damping.

CHAPTER 1. GENERAL REMARKS

In 1959, it was stated in reference 5 that the damping of aerodynamic /5* vibrations was still insufficiently understood and that more research would be required to improve our knowledge of the subject. Nevertheless, investigations prior to 1959 by either considering the fluids as nonviscous and the flow as exempt from detachment (refs. 9, 18, 33), or by introducing vortical singularities (refs. 38, 40) and by outlining a mechanism of the intervention of detachments (ref. 40) have shown that such research would have to go beyond the case of combined flexure and torsion which was carefully investigated in regard to airfoils (refs. 23, 44). Incompletely explained facts (refs. 1, 13, 16) did furnish some experimental support. Since 1959, ideas related to those developed below have been experimented (refs. 21, 49) and the question of coupling between blades was reexamined (ref. 19).

We know that the use of a distribution of aerodynamic singularities makes it possible in a general manner to describe fluid flow in the blading of a turbine (refs. 30, 32, 36, 37, 45, 48). This method was adapted to the specific problem of the evaluation of aerodynamic stresses in steady state on the basis of the velocity diagram schematically representing the operational behavior of the blading under consideration.

Regarding evaluation of the mechanical stresses, this is limited to bending stress, where the method of concentrated mass has been adopted which makes it possible to solve the problems strictly. Provided a distribution of mass of sufficiently large number is selected, it is possible to account for the centrifugal forces, the inertial forces, and the elastic reactions developed simultaneously during the vibratory behavior of the blading (refs. 23, 43).

1.1 Investigation of Damping Without Aerodynamic Detachment

Specifically, the analytic representation of flow is bidimensional and constructed by means of a family of identical vortices each centered on a cascade profile adjusted in conformity with the datum of the velocity diagram. The elementary vortex of this family is numerically characterized by the /6 expression of the circulation γ of the velocity vector around the respective profile as a function of

(1) the cascade pitch τ;

---

*Numbers given in margin indicate pagination in original foreign text.

(2) the angle of inclination α in relation to the cascade with the geometric mean W_m of the relative velocities at infinity both upstream and downstream;

(3) the specific weight of the fluid m_s;

(4) the expansion (or compression) Δp across the cascade

$$\gamma = \frac{\tau \Delta p}{m_s \cdot W_m \cdot \cos \alpha}.$$

This emphasizes the predominant role of the viscosity forces which generate circulation within the boundary layer. The application of the Euler theorem to the datum of the velocity diagram makes it possible, moreover, to reproduce the results obtained by the Blasius integration and confirms that the combined vortices are taken into account while neglecting the influence of the free vortices released in the wake of the profiles, i.e., that the aerodynamic problem is treated for infinitely long blades.

By admitting the different approximations above as a whole, we then continue from formulation of an equation for steady state to the formulation of an equation for an alternate transient regime on the following reasoning:

(a) blade vibration is expressed by an oscillation of the profile in relation to a system of axes (0) linked to the turbine rotor;

(b) the absence of detachment implies that any fluid molecule M reaching the leading edge remains in contact with the profile and consequently its velocity in the system of axes (0) is the geometric sum of the profile velocity of flow and velocity of oscillation;

(c) the trajectory of a molecule M is therefore different in alternate transient regimes from that in a steady regime, and everything takes place in regard to the conditions at the limits to infinity upstream and downstream as if the angle of fluid deviation inducing expansion or compression, i.e., the angle at the apex ψ of the velocity diagram, underwent a variation $\Delta\psi$ whose amplitude can be calculated as a function of time;

(d) recourse to the continuity of circulation γ makes it possible to express, on the basis of these considerations, the oscillation of γ as a function of time from which we can deduce the expression of the aerodynamic stresses in an alternate transient regime; when γ_0 designates the mean value of the circulation γ calculated for steady regime, we then use γ in the form

$$\gamma = \gamma_0 + \gamma_1 \cdot \sin(\omega t + j) = \gamma_0 + \frac{d\gamma}{d\psi} \Delta\psi.$$

$\Delta\psi$ is expressed as a function of the displacement of the profile between the instant t when the molecule M encounters the leading edge and the instant t + td when it leaves the trailing edge, using a very simple geometric infinitesimal analysis

$$\Delta\psi = -k_0 \{\Delta y\}_{t}^{t+td}.$$

This supposes that, at a given instant t, each molecule participating in the constitution of the boundary layer behaves in regard to the pressure stresses on the profile as if it were to undergo the fluid deviation $\Delta\psi(t, t + td)$ during its contact with the profile. However, at the instant $t + \Delta t$, certain of the molecules active at the instant t have lost contact with the profile whereas others are now in contact with it, and the new grouping unanimously behaves as if each individual were to undergo the deviation $\Delta\psi(t + \Delta t, t + \Delta t + td)$ while it is in contact with the profile. We therefore adopt the postulate that all the particles constituting the boundary layer at a given instant become a solid mass due to the action of viscosity. /7

Admitting further that the position of the profile in relation to the axes (O) can be defined by a sinusoidal function of time

$$y = (y)_M \sin \omega t$$

where the derivative $\frac{d}{dt}\left[(y)_M\right]$ is limited upward by a negligible quantity, we proceed by identification

$$\gamma_1 \cdot \sin(\omega t + j) = -k_1 \frac{\partial \gamma}{\partial \psi} \cdot (y)_M \{\sin(\omega [t + td] - \sin \omega t)\},$$

and consequently

$$\gamma = \gamma_0 + F(\tau, W_m, \Delta p) \cdot \frac{\omega c_d}{W_m} \cdot \cos\left(\omega t + \frac{\omega c_d}{2 W_m}\right),$$

where c_d designates the chord of the profiles.

We finally retain the expression of the resultant of the aerodynamic stresses in steady regime in the second member of the equation for the vibrations. In the first member, we show two terms which together represent the oscillation of the aerodynamic resultant around its mean value as a function of y and $\frac{dy}{dt}$. The term in y introduces a variation of the characteristic frequency. The term in $\frac{dy}{dt}$ introduces a damping increasing specifically with the relative pitch $\frac{\tau}{c_d}$, at the ratio of specific weight of the fluid and of the blade material as well as with the mean velocity W_m. Such an indication of

tendency entirely conforms with experience for cases of slight incidence and moderate flow velocities. The numerical values obtained are greater than those currently observed but the orders of magnitude are comparable. This demonstrates in addition that neither the interaction between adjacent blades nor the characteristic damping of the material are predominant.

The actual investigation of the damping is the subject of Chapter 5. Chapters 2 and 3 make it possible to establish a logical base of the investigation for the transient regime according to a new process which gives a physical meaning to the nonuniform potential functions (refs. 4, 12, 20, 47). Chapter 4 is intended to show, prior to investigation of the damping, that the interaction between adjacent blades is not systematically the cause of instabilities (ref. 49).

1.2 Investigation of Damping in the Presence of Aerodynamic Detachment

The reasoning explained above applies integrally, with this difference: /8 the molecule M loses contact with the profile before reaching the trailing edge. This thickens the wake and reduces the angle ψ, consequently the circulation γ and specifically the damping previously demonstrated.

A. Steady-state Regime

The perfect detachment can be defined as cancellation of the angle ψ itself considered as a first order infinitely small angle (slight incidence). In this circumstance, the molecule M exits from the blading at a point staggered in relation to the profile of a quantity

$$(\Delta y) \text{ total permanent detachment} = \frac{c_d \cdot |\psi|}{\cos \theta_1};$$

which is an expression in which θ_1 designates the inclination of the profile chord in relation to the cascade's perpendicular direction.

The detachment to be considered when instead the flow is almost perfect is one where the molecule M loses contact with the profile only at a small distance a_d from the profile tip. It therefore leaves the blading at a point staggered in relation to the profile of a quantity

$$(\Delta y) \text{ partial permanent detachment} = \frac{a_d \cdot e_p}{\cos \theta_1};$$

designating the angle between the relative velocity at the profile tip (downstream at infinity), as obtained in nondetached flow, and the relative velocity at the point where the molecule M loses contact with the profile in detached flow.

We then introduce the turbulence in the channel constituted by two consecutive blades by writing that the ratio between the two quantities formulated above depends only on the Reynolds number assigned to the idea of a hydraulic diameter D_h

$$\mathrm{Re} = \frac{W_m D_h}{\nu}$$

(which allows us to introduce the kinematic viscosity of the fluid ν). It is then shown that the number Re is the product of two quantities, one of which depends only on the velocity diagram, on the profile and on the fluid and where the other characterizes the cascade effect (relative pitch and elongation of the blades). We therefore have /9

$$\frac{a_d \cdot e_p}{\cos \theta_1} = \frac{c_d |\psi|}{\cos \theta_1} \cdot d_p(\mathrm{Re})$$

or

$$a_d \cdot e_p = c_d |\psi| \cdot d_p(\mathrm{Re}).$$

The function $d_p(\mathrm{Re})$ depends on the profile form. We propose to determine this during wind-tunnel experimentation of the cascade and under permanent flow.

B. Alternate Transient Regime

The oscillating motion of the blade has a tendency both to reattach the detached flow lines and/or to aggravate the detachment (refs. 38, 40, 49) in such manner that the double amplitude of the fluid oscillation is less than the blade oscillation amplitude. At least approximately, we propose to take into account this phenomenon and, specifically, the local acceleration in the fluid at the points for which the profile oscillation velocity in relation to the axes (0) is zero. We will do so by stating that there is complete cancellation of detachment when elongation is maximum and in a direction opposite to the fluid deviation, and where the mean point of fluid oscillation at the blading exit must necessarily be the point at which the molecule M leaves the blading in partially detached steady flow.

This reasoning and the supplementary hypothesis lead us to adopt, in order to define the oscillation of the circulation, the expression

$$\cdot \left\{ (y)_M - \frac{c_d \cdot |\psi|}{\cos \theta_1} \cdot d_p(\mathrm{Re}) \right\} \sin \omega t$$

in contrast to the sinusoidal function

$$y = (y)_M \cdot \sin \omega t$$

which defines the oscillation of the profile and was utilized to express the oscillation of γ in the absence of detachment.

Finally, in the equation for the vibrations and in the second member, we show a new term dependent on time having the form

$$k_2 \cdot \cos\left(\omega t + \frac{\omega c_d}{2 W_m}\right),$$

which may give rise to an asymptotic vibration maintained by the fluid, so that we may observe an apparently negative damping coefficient and, in particular, a rupture due to blade fatigue. By analogy with the behavior of a plane wing, it is clear that the "instabilities," which the preceding formulas cannot show except by possible discontinuity of the function $d_p(Re)$, correspond /10

to the generalized loss of lift responsible for the stalling in aircraft (refs. 1, 28).

1.3 Results Obtained

We then state that "for a given flow velocity and at the end of an invariable interval starting with the instant of release into the wind, there correspond successively, to increasing values of the incidence, positive, zero, and finally negative values of the damping coefficient; under the same conditions, the same phenomenon, due to the progressive increase of turbulence in the blade cascade channels, is produced under constant incidence if the incident velocity is increased."

In conclusion, the reader is asked to remember that in the field of blade vibration as well as in the better known flight mechanics and mechanics of the displacement of objects on dry ground, the imperceptible role of friction determines the trend of the observable phenomena.

CHAPTER 2. INVESTIGATION OF FLOW

2.1 Analytical Representation

Figure 1 shows the xyu axes selected for evaluating the stresses. /11
The direction of the u axis parallel to the axis of machine rotation is that of the flow. The x axis is radial in accordance with the blade elongation. The y axis is oriented along the tangential velocity of the rotor; the trihedron xyu is direct; the xy plane is that of the rotor and the yu plane is a meridian plane of the machine; the xy and yu axes are also direct.

In developing the rim which carries the blades, we obtain a cascade and a plane in which we consider, holding certain restrictions, that the bi-dimensional flow is representative of the real flow, and such a flow can be calculated by means of nonuniform aerodynamic potential functions in symbolizing the cascade as a succession of identical vortices each representing a cascade profile.

The complex plane coincides with the flow plane; the OX axis of this plane is directed in accordance with the geometric mean W_m of the relative velocity at the intake of the blading W_1 and of the relative velocity at the exit of the

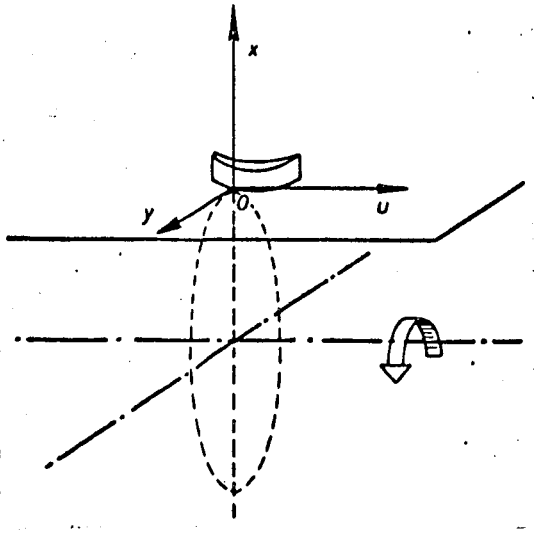

Figure 1

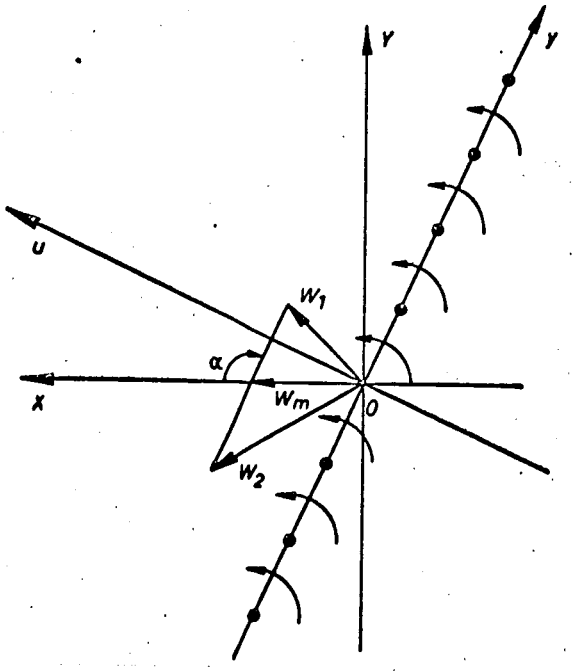

Figure 2

blading W_2. The line of vortices is inclined at the angle α on the axis /12

Ox; the axis OY is oriented as is axis Oy so that the positive direction of rotation in the complex plane is the negative direction in the plane yOu. The velocity diagram which constitutes the initial datum is inscribed in this geometric configuration as indicated in figure 2.

The corresponding potential function is written as

$$\Phi = W_m \cdot z - \frac{i \cdot \gamma}{2\pi}\left\{Lz + \sum_{n=-N}^{n=+N} L\left(z - i \cdot n \cdot \tau \cdot e^{i\alpha}\right)\right\}; \qquad (1)$$

where z is the affix of the complex variable X + iY;
(γ) is the circulation of the relative velocity vector around a vortex;
n is the order number of the vortex counted positively along OY and negatively in the inverse direction;
(τ) is the distance between two consecutive vortices;
2 N + 1 is the number of profiles of the cascade.

2.2 Examination of this Representation

A. Examination of the Isolated Vortex and Significance of the Sign of (γ)

Exploration of the field of velocities generated by an isolated vortex makes it possible to better understand the result obtained by geometric composition for the whole cascade.

The complex potential linked to the vortex of order (0) is given by the formula /13

$$\Phi_0 = -\frac{i\gamma}{2} \cdot Lz.$$

The corresponding complex velocity is

$$\frac{d\Phi_0}{dz} = W_{x_0} - iW_{y_0} = \frac{i \cdot \gamma}{2\pi z} = -\frac{i \cdot \gamma}{2\pi \cdot r \cdot (\cos\theta + i \cdot \sin\theta)}.$$

where W_x and W_y are the components of aerodynamic velocity generated by the vortex of order (0);
r and θ are the polar coordinates of the point at which we calculate the aerodynamic velocity.

$$W_{x_0} = -\frac{\gamma \cdot \sin\theta}{2\pi r}; \qquad W_{y_0} = \frac{\gamma \cdot \cos\theta}{2\pi \cdot r}.$$

This aerodynamic velocity is perpendicular to the vector radius $\overrightarrow{OM}$ (fig. 3) and, by using the corresponding circulation along the circumference (0) with radius r, we find

$$\int_0 \vec{W} \cdot \vec{ds} = \int_0^{2\pi} \frac{\gamma \cdot r \cdot d\theta}{2\pi \cdot r} = \gamma. \qquad (2)$$

We note that if γ is negative the aerodynamic velocity circulates in the negative direction of rotation, which permits axis OY and axis OX to coincide by a 90° rotation. We also note that if γ is positive the aerodynamic velocity circulates in the positive direction of rotation. The result is that, if the movement generated by the respective vortex is superimposed on a motion of translation directed along OX, the transverse impulsion will combine with the vortex along OY in the first case and will be in the inverse direction in the second case. Since OY has the same direction as Oy, this impulsion has the /14 direction of motion of the rotor when γ is negative (operation as turbine) and the contrary direction to that of the motion when γ is positive (operation as compressor).

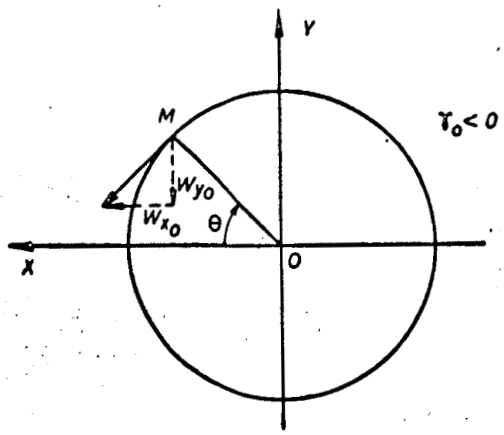

Figure 3

B. Calculation of Velocity at any Point of the Flow Resulting from the Combination of the Various Vortical Potential Functions and of Translation Parallel to OX

Formula (1) above satisfactorily corresponds to this definition. To facilitate manipulation, it can be transformed using relation

$$\prod_{n=1}^{n=\infty} z \cdot (z^2 - \tau^2 \cdot e^{2i\alpha}) \dots (z^2 - n^2 \cdot \tau^2 \cdot e^{2i\alpha})$$

$$= \prod_{n=1}^{n=\infty} \left\{ \frac{1}{\pi} \cdot \tau \cdot e^{L\alpha} \cdot (\tau)^2 e^{2i\alpha} \dots n^2 \cdot (\tau)^2 \cdot e^{2i\alpha} \dots \right\} \cdot i \cdot \sin \frac{\pi z}{\tau \cdot e^{i\alpha}}$$

which becomes by logarithmic treatment

$$\lim_{n\to\infty} \left\{ Lz + \sum_{-n}^{+n} L(z \cdot i \cdot n \cdot e^{i\alpha}) \right\} = Lz + \sum_{-N}^{+N} L(z - i \cdot n \cdot e^{i\alpha}) + \lim_{n\to\infty} \sum_{N+1}^{n} L(z^2 + n^2 \tau^2 \cdot e^{2i\alpha});$$

$$\lim_{n\to\infty} \left\{ L\left[\frac{1}{\pi} \cdot \tau \cdot e^{i\alpha} \cdot \tau^2 \cdot e^{2i\alpha} \dots \right] \right\} + L\left(i \cdot \sin \frac{\pi \cdot z}{\tau \cdot e^{i\alpha}} \right)$$

$$= \frac{2\pi}{i \cdot \gamma} (W_m \cdot z - \Phi) + \lim_{n\to\infty} \left\{ \sum_{n=N+1}^{n} L(z^2 + n^2 \cdot \tau^2 \cdot e^{2i\alpha}) \right\}$$

and suggests the use, instead of the function Φ, of the new potential function

$$\Phi_s = W_m \cdot z - \frac{i\gamma}{2\pi} \cdot L\left(i \cdot \sin \frac{\pi z}{\tau \cdot e^{i\alpha}}\right), \tag{3}$$

and consequently

$$L\left(i \cdot \sin \frac{\pi z}{\tau \cdot e^{i\alpha}}\right) \frac{2\pi}{i \cdot \gamma} (W_m z - \Phi_s);$$

$$\lim_{n\to\infty} \left\{ L \frac{\tau \cdot e^{i\alpha} \cdot \tau^2 \cdot e^{2i\alpha} \ldots n^2 \cdot \tau^2 e^{2i\alpha}}{\pi} \right\} + \frac{2\pi}{i \cdot \gamma} (W_m \cdot z - \Phi_s)$$

$$= \frac{2\pi}{i \cdot \gamma} (W_m \cdot z - \Phi) + \lim_{n\to\infty} \sum_{N+1}^{n} L\,(z^2 + n^2 \cdot e^{2i\alpha})$$

and finally

$$\left\{ L \frac{\tau \cdot e^{i\alpha} \cdot \tau^2 \cdot e^{2i\alpha} \ldots N^2 \cdot \tau^2 \cdot e^{2i\alpha}}{\pi} \right\} + \frac{2\pi}{i \cdot \gamma} (\Phi - \Phi_s)$$

$$= \lim_{n\to\infty} \sum_{N+1}^{n} L\left(1 + \frac{z^2}{n^2 \cdot \tau^2 \cdot e^{2i\alpha}}\right).$$

However, the second member of the equation thus obtained is no other /15 than the expression of a series which converges like the series $\frac{z^2}{n^2 \cdot \tau^2 \cdot e^{2i\alpha}}$ over the entire complex plane, provided N is sufficiently large. In addition, its sum is as much closer to the remainder of the series $\frac{z^2}{n^2 \cdot \tau^2 \cdot e^{2i\alpha}}$ terminated at the nth term, and consequently as much lower as N is greater.

It therefore seems that the functions Φ and Φ_s differ in practice only by a constant and that the derivative $\frac{d\,\Phi_s}{dz}$ can represent the desired field of aerodynamic velocities with a controllable approximation.

C. Exploration of the Field of Aerodynamic Velocities

We have

$$\frac{d\Phi_s}{dz} = W_x - iW_y = W_m - \frac{i \cdot \gamma}{2 \cdot \tau \cdot e^{i\alpha}} \operatorname{cotg} \frac{\pi z}{\tau \cdot e^{i\alpha}}$$

and state

$$Z = \frac{\pi z}{\tau \cdot e^{i\alpha}},$$

and consequently

$$\operatorname{cotg} Z = \frac{e^{2iz} + 1}{e^{2iz} - 1}$$

to explore the plane of flow by means of real variables, i.e.,

λ = vectorial modulus (vector radius $r = \frac{\lambda \cdot \tau}{\pi}$),

θ = azimuthal argument,

that is

$$z = \frac{\lambda \cdot z \cdot e^{i\theta}}{\pi}$$

and consequently

$$Z = \lambda \cdot e^{i(\theta - \alpha)}$$

with

$$e^{2iz} = e^{2i\{\lambda\cos(\theta-\alpha)+i\cdot\lambda\sin(\theta-\alpha)\}},$$

$$h_0 = e^{-2\lambda\sin(\theta-\alpha)},$$

$$a_0 = \cos\{2\lambda\cos(\theta-\alpha)\}; \qquad b_0 = \sin\{2\lambda\cos(\theta-\alpha)\},$$

and then

$$\operatorname{cotg} Z = i\frac{h_0(a_0 + ib_0) + 1}{h_0(a_0 - ib_0) - 1} = \frac{2h_0 b_0 + i(h_0^2 - 1)}{h_0^2 - 2h_0 a_0 + 1}$$

and finally

$$\frac{i\cdot\gamma}{2\cdot\tau\cdot e^{i\alpha}} = \frac{i\cdot\gamma}{2\cdot\tau\cdot(\cos\alpha + i\sin\alpha)} = \frac{\gamma}{2\tau}(\sin\alpha + i\cos\alpha),$$

$$W_x - iW_y = W_m - \frac{\gamma}{2z}(\sin\alpha + i\cdot\cos\alpha)\frac{2h_0 b_0 + i(h_0^2 - 1)}{h_0^2 - 2h_0 a_0 + 1},$$

where W_x and W_y designate, respectively, the components along X and Y of the relative velocity W at the respective point /16

$$\begin{cases} W_x = W_m - \dfrac{\gamma}{2\tau}\dfrac{(h_0^2 - 1)\cos\alpha - 2h_0 b_0 \sin\alpha}{h_0^2 - 2h_0 a_0 + 1}, \\ W_y = \dfrac{\gamma}{2\tau}\dfrac{2h_0 b_0 \cos\alpha + (h_0^2 - 1)\sin\alpha}{h_0^2 - 2h_0 a_0 + 1}. \end{cases} \tag{4}$$

D. Arrangement of Velocity Diagram

We here verify, a posteriori, that the conditions at the limits to the infinite are sufficiently satisfied by the function Φ_S.

1. At infinity upstream

Figure 4 resumes the passage to the limit given below

$$\pi + \alpha > \theta > \alpha,$$

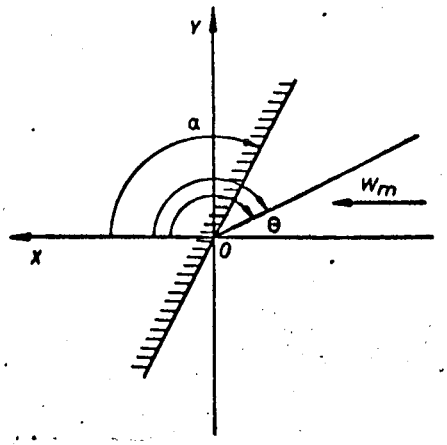

Figure 4

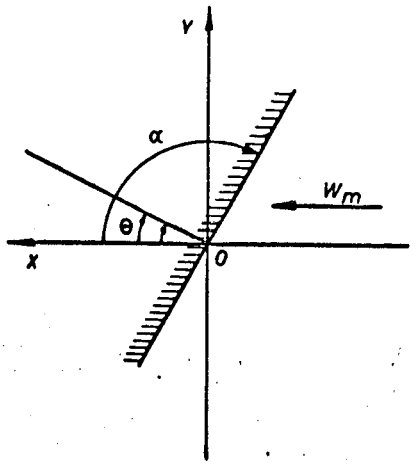

Figure 5

accordingly sin $(\theta - \alpha) > 0$ and $h_0 \to 0$ when $\lambda \to \infty$.

$$W_x \to W_m - \frac{\gamma}{2\tau}\cos\alpha,$$

$$W_y \to -\frac{\gamma}{2\tau}\sin\alpha.$$

2. At infinity downstream

Figure 5 resumes the passage to the limit given below

$$-(\pi - \alpha) < \theta < \alpha,$$

accordingly sin $(\theta - \alpha) < 0$ and $h_0 \to \infty$ when $\lambda \to \infty$.

$$W_x \to W_m + \frac{\gamma}{2\tau}\cos\alpha,$$

$$W_y \to \frac{\gamma}{2\tau}\sin\alpha.$$

These two results make it possible to construct figure 6. When circulation is negative, the arrangement of the velocity diagram corresponds to the operation of a turbine and when the circulation is positive, the arrangement of the velocity diagram corresponds to operation as a compressor. /17

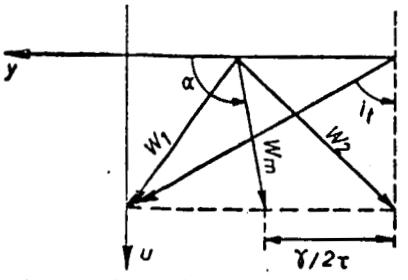

Figure 6

E. Calculation of the Circulation Determining Flow as a Function of the Initial Elements of the Velocity Diagram

Figure 7 introduces the following geometric parameters not mentioned earlier:

i_t is the inclination of absolute velocity at the intake along the turbine axis;

m is the inclination of the relative velocity W_1 (theoretically at infinity upstream) along the turbine axis;

V_1 is intensity of the absolute velocity at the intake (theoretically at infinity upstream);

ψ is the deviation of the fluid due to the blading;

$\overrightarrow{\Delta W}$ is the geometric difference between the relative velocities downstream and upstream;

these make it possible to write the following relations

$$\frac{\gamma}{\tau} = +\Delta W = -W_1 \frac{\sin\psi}{\sin\left(\frac{\pi}{2} + m - \psi\right)} = -W_1 \frac{\sin\psi}{\cos(\psi - m)}, \tag{5}$$

$$\frac{V_1 \cos i_t}{W_1} = \sin\left(m + \frac{\pi}{2}\right) = \cos m, \tag{6}$$

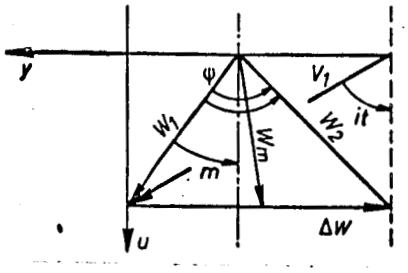

Figure 7

so that

$$\gamma = -\tau \cdot V_1 \cdot \frac{\cos i_l \cdot \sin \psi}{\cos (\psi - m) \cdot \cos m}. \tag{7}$$

This expression of the circulation is valid both for the turbines ($\gamma < 0$) and for the compressors ($\gamma > 0$) on the condition of counting algebraically in the system of xyu axes. It is obviously assumed, moreover, that ψ satisfies the inequalities /18

$$\begin{cases} \psi > 2m, \\ \gamma \cdot m < 0, \end{cases} \tag{8}$$

which limit the examination to real cases of operation and to a rotation of the machine in the direct trigonometric sense.

2.3 Numerical Calculation and Determination of the Limit Conditions at Finite Distance

We have given a numerical example so as to illustrate the conclusions of Section 2.2 and make it possible to apply them to the calculation of the aerodynamic forces in steady and transient regimes.

The elements of this numerical application are represented in figure 8; i.e.,

$$i_l = \frac{\pi}{3}; \qquad V_1 = W_m \cdot \sqrt{3}; \qquad W_1 = W_m;$$

$$m = +\frac{\pi}{6}.$$

The pitch of the blading τ is taken equal to unit length. It will easily be seen that the value of α to be introduced in formula (4) is

$$\alpha = \frac{2\pi}{3};$$

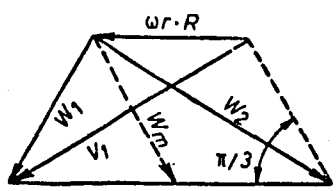

Figure 8

by taking into account the relation

$$\frac{\gamma}{2\tau} = -W_m$$

we deduct from the equations (4) /19

$$W_x = W_m\left(1 + \frac{2h_0 b_0\sqrt{3} + h_0^2 - 1}{2(h_0^2 - 2h_0 a_0 + 1)}\right),$$

$$W_y = W_m \frac{2h_0 b_0\sqrt{3}(h_0^2 - 1)}{2(h_0^2 - 2h_0 a_0 + 1)}.$$

A. Determination of Zero-Velocity Points

Their coordinates are solutions of the system of equations

$$\begin{cases} 2(h_0^2 - 2h_0 a_0 + 1) + 2h_0 b_0\sqrt{3} + h_0^2 - 1 = 0; & (9) \\ \sqrt{3}(h_0^2 - 1) - 2h_0 b_0 = 0. & (10) \end{cases}$$

By eliminating h_0^2 between equations (9) and (10), we obtain

$$h_0 = \frac{1}{a_0 - b_0\sqrt{3}} = e^{-2\lambda\sin(\theta-\alpha)} > 0,$$

so that, from equation (10)

$$b_0 = \frac{b_0}{\sqrt{3}} + \sqrt{\frac{b^2}{3} + 1}.$$

If we desire a_0 and b_0 in the form

$$a_0 = \cos|2\lambda\cos(\theta - \alpha)| = \cos A; \qquad b_0 = \sin|2\lambda\cos(\theta + \alpha)| = \sin A,$$

so that

$$\sin A + \sqrt{\sin^2 A + 3} = \frac{\sqrt{3}}{2}\frac{1}{\frac{1}{2}\cos A - \frac{\sqrt{3}}{2}\sin A} = \frac{\sin\frac{\pi}{3}}{\cos\left(\frac{\pi}{3} + A\right)};$$

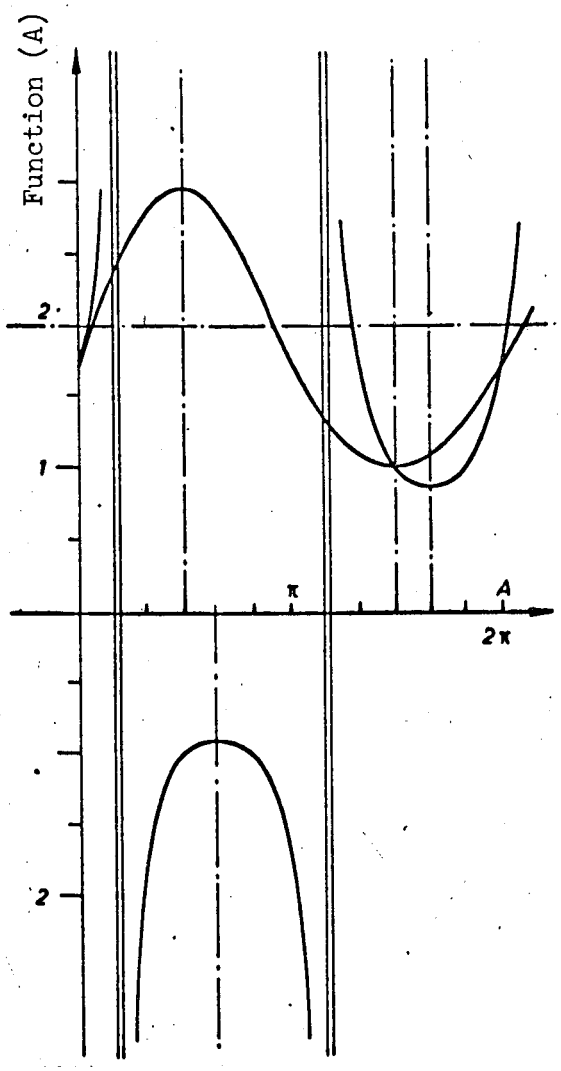

Figure 9

we find an equation in A whose roots are

$$A_1 = 2k'_1 W \text{ (where } k'_1 \text{ is whole, positive, negative or zero)} \qquad (11)$$

$$A_2 = \frac{3\pi}{2} + 2k'_2 \text{ (where } k'_2 \text{ is whole, positive, negative or zero)} \qquad (12)$$

These roots are shown in figure 9. From equation (11), we can deduce the first series of values of

$$2\lambda \cos(\theta - \alpha) = 2k'_1\pi, \text{ that is, } \lambda = \frac{k'_1\pi}{\cos(\theta - \alpha)}$$

and

$$h_0 = \frac{1}{a_0 - b_0\sqrt{3}} = 1 = e^{-h'_1 \pi \cdot \mathrm{tg}(\theta - \alpha)}.$$

These are parasite solutions

$$\theta = \alpha + k'\pi; \qquad \lambda = \pm k'_1 \pi; \qquad r = \pm k'_1 \cdot \tau,$$

contained in the initial formula (3) and corresponding to the indeterminate velocity W immediately adjacent to the vortices symbolizing the blades of the cascade. /20

It now appears that the calculated flow does not exactly represent reality in the immediate vicinity of the profiles. We shall see farther below that this has no importance in the calculation of the stresses and instead goes hand in hand with the possible generalization of this calculation, independent of the form of the profiles.

From equation (12) we can deduce a second series of values of λ

$$2\lambda \cos(\theta - \alpha) = \frac{3\pi}{2} + 2 \cdot k'_2 \cdot \pi, \quad \text{or} \quad \cos(\theta - \alpha) = \frac{3\pi}{4\lambda} + \frac{k'_2}{\lambda}$$

with

$$h_0 = \frac{1}{a_0 - b_0\sqrt{3}} = \frac{1}{\sqrt{3}}$$

$$\mathrm{Log}\, h_0 = -2\lambda \sin(\theta - \alpha) = -\frac{1}{2}\mathrm{Log}\, 3.$$

$$\lambda = \frac{\mathrm{Log}\, 3}{4 \sin\left(\theta - \frac{2\pi}{3}\right)}; \qquad r = \frac{\tau\, \mathrm{Log}\, 3;}{4\pi \sin\left(\theta - \frac{2\pi}{3}\right)};$$

$$\mathrm{tg}\left(\theta - \frac{2\pi}{3}\right) = \frac{\mathrm{Log}\, 3}{\pi} \frac{1}{3 + 4k'_2}.$$

To each whole, positive, negative or zero value of k'_2 there corresponds a zero-velocity point located in the proximity of one of the vortices symbolizing the blades of the cascade. The coordinates of the point closest to the vortex located at the origin are obtained with $k'_2 = -1$, that is /21

$$\operatorname{tg}\left(\theta-\frac{2\pi}{3}\right)=-\frac{\operatorname{Log}3}{\pi}=-0.3497,$$

$$\sin\left(\theta-\frac{2\pi}{3}\right)=-0.3300;$$

$$\theta=120^{\circ}-19^{\circ}16'=100^{\circ}44',$$

$$r=\frac{-\operatorname{Log}3}{4\cdot 0.330}=-0.2649.$$

B. Evolution of Velocity in the Channels Along the Rotor Periphery

The formulas become simplified as indicated below

$$\theta=\alpha;\qquad \sin(\theta-\alpha)=0;\qquad h_0=1;\qquad 2\lambda\cos(\theta-\alpha)=A=2\lambda.$$

so that it is easy to prepare table 1, which gives the desired evolution.

C. Evolution of Velocity Parallel to the Turbine Axis

The points at which the velocities producing this evolution are calculated are taken at the intersection of axis Ou and circles with the respective radii

$$r=0.2;\qquad r=0.4;\qquad r=0.6;\qquad r=0.8.$$

The corresponding calculations are entered in tables 2 and 3.

D. Systematic Trace of the Flow Line Passing Through a Given Point

We assimilate the desired curve to a polygon. By multiplying the sides of this polygoh, it is possible to reach any predetermined precision. /24

Figure 9A furnishes the indication of the method. The angles V_n are those formed by the vector radius of the point of order $n(r_n, \theta_n)$ with the tangent at this point, and the angles B_n are those formed by the vector radius of the point of order n with the tangent at the point of order $n-1(r_n-1, \theta_n-1)$, so that we have the relations

$$\frac{r_{n-1}}{\sin(B_{n-1})}=\frac{r_n}{\sin(V_{n-1})},$$

$$d\theta_n=\theta_n-\theta_{n-1},$$

$$B_{n-1}=V_{n-1}-d\theta_n,$$

TABLE 1. VORTICAL AXES ($\theta - \alpha = 0$).

	0,2 . τ	0,4 . τ	0,5 . τ	0,6 . τ	0,8 . τ	0,9 . τ
$\lambda = \frac{\pi \cdot r}{\tau}$	0,2 · π	0,4 · π	0,5 · π	0,6 · π	0,8 · π	0,9 · π
2λ	0,4 · π	0,8 · π	1 · π	1,2 · π	1,6 · π	1,8 · π
$A = 2 \cdot \lambda \cdot \frac{180}{\pi}$	72°	144°	180°	216°	288°	324°
$a_0 = \cos A$	0,3090	— 0,8090	— 1	— 0,8090	— 0,3090	0,8090
$b_0 = \sin A$	0,9511	0,5878	0	— 0,5878	— 0,9511	— 0,5878
$2 b_0 h_0 + \sqrt{3} (h_0^2 - 1)$	1,9022	1,1756	0	— 1,1756	— 1,9022	— 1,1756
$2 a_0 h_0$	0,6180	— 1,6180	— 2	— 1,6180	0,6180	1,6180
$2 (h_0^2 + 1 - 2 a_0 h_0)$	2,7640	7,2360	8	7,2360	2,7640	0,7640
$2 b_0 h_0 \sqrt{3}$	3,300	2,040	0	— 2,040	— 3,300	— 2,040
$2 (h_0^2 + 1 - 2 a_0 h_0) + 2 h_0 b_0 \sqrt{3} - (1 - h_0^2)$	6,064	9,276	8	5,196	— 0,536	— 1,276
$\text{tg } T = \frac{W_y}{W_x}$	0,314	0,127	0	— 0,226	3,555	0,9210
T	17°30	7°30	0	— 12°30	— 105°30	— 137°30

Commas in all tables represent decimal points.

TABLE 2. AXES INCLINED AT $+\frac{\pi}{3}$ ON POSITIVE Ou AXIS $\left(\alpha = -\frac{\pi}{3}\right)$.

r	$0{,}2 \cdot \tau$	$0{,}4 \cdot \tau$	$0{,}6 \cdot \tau$	$0{,}8 \cdot \tau$
$\lambda = \frac{\pi \cdot r}{\tau}$	$0{,}2 \cdot \pi$	$0{,}4 \cdot \pi$	$0{,}6 \cdot \pi$	$0{,}8 \cdot \pi$
2λ	$0{,}4 \cdot \pi$	$0{,}8 \cdot \pi$	$1{,}2 \cdot \pi$	$1{,}6 \cdot \pi$
$A = 2 \cdot \lambda \cdot \cos\frac{\pi}{3} \cdot \frac{180}{\pi}$	36°	72°	108°	144°
$a_0 = \cos A$	0,8090	0,3090	— 0,3090	— 0,8090
$b_0 = \sin A$	0,5878	0,9511	0,9511	0,5878
$-2 \cdot \lambda \cdot \sin\left(-\frac{\pi}{3}\right)$	1,0885	2,177	3,265	4,354
$e^{-2\cdot\lambda\cdot\sin(0-\alpha)} = h_0$	2,969	8,817	26,182	77,804
$2 b_0 h_0$	3,4903	16,771	49,803	91,466
$\sqrt{3}\,(1 - h_0^2)$	— 13,537	— 123,906	— 1 185,60	— 10 483,0
$2 b_0 h_0 + \sqrt{3}\,(1 - h_0^2)$	— 10,0467	— 116,135	— 1 135,797	— 10 391,534
$2 a_0 h_0$	4,804	5,448	— 16,1804	— 125,826
$2 (h_0^2 + 1 - 2 a_0 h_0)$	10,022	146,568	1 405,3208	12 360,452
$2 b_0 h_0 \sqrt{3}$	6,0453	29,048	86,262	158,422
$2 (h_0^2 + 1 - 2 a_0 h_0) + 2 b_0 h_0 \sqrt{3} - (1 - h_0^2)$	23,8819	252,348	2 176,063	18 571,274
T	— 23°	— 24°30	— 27°30	— 29°

TABLE 3. NEGATIVE Ou AXIS $\left(\theta - \alpha = \frac{\pi}{2}\right)$.

r	$0{,}2\ (\tau)$	$0{,}4\ (\tau)$	$0{,}6\ (\tau)$	$0{,}8\ (\tau)$
$\lambda = \frac{\pi \cdot r}{\tau}$	$0{,}2 \cdot \pi$	$0{,}4 \cdot \pi$	$0{,}6 \cdot \pi$	$0{,}8 \cdot \pi$
2λ	$0{,}4 \cdot \pi$	$0{,}8 \cdot \pi$	$1{,}2 \cdot \pi$	$1{,}6 \cdot \pi$
$A = 2\lambda \cdot \cos\frac{\pi}{2} \cdot \frac{180}{\pi}$	0	0	0	0
$a_0 = \cos A$	1	1	1	1
$b_0 = \sin A$	0	0	0	0
$-2\lambda \cdot \sin\frac{\pi}{2}$	— 1,25664	— 2,51328	— 3,76992	— 5,02656
$e^{-2\cdot\lambda\cdot\sin(\theta-x)} = h_0$	0,2846	0,08100	0,02305	0,006565
$2 b_0 h_0$	0	0	0	0
$\sqrt{3}\,(1 - h_0^2)$	1,5918	1,7207	1,7311	1,732
$2 a_0 h_0$	0,5692	0,16200	0,04610	0,013130
$2 (h_0^2 + 1 - 2 a_0 h_0)$	1,0236	1,68913	1,90886	1,97383
$2 (h_0^2 + 1 - 2 a_0 h_0) - (1 - h_0^2)$	0,10460	0,69570	0,90939	0,97387
tg T	15,218	2,473	1,904	1,778
T	86°15′	68°	62°30′	60°30′

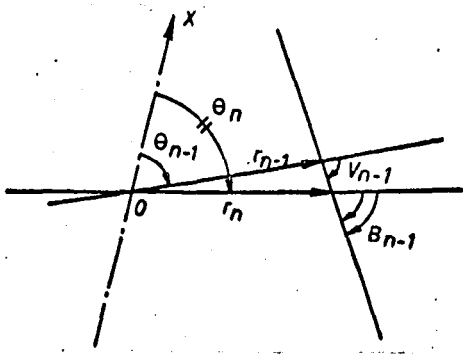

Figure 9A

from which we derive the recurrence formula of the vector radii as a function of the preselected arguments;

$$r_n = r_{n-1} \frac{\sin (V_{n-1})}{\sin (V_{n-1} - d\,\theta_n)}.$$

From this it is easy to deduce table 4, in which $d\theta$ are 10° or 5°, which gives the elements of the desired trace. This table is referenced to the flow line (c) separating the velocity field around the blade with affix Z_n from the velocity field around the blade with affix Z_{n-1}.

E. Determination of Limit Conditions at Finite Distance. Trace of Blade Profile

Since the distribution of vortices is given and the velocity field is organized in accordance with a family of flow lines, the limit conditions at finite distance can be satisfied in only one manner, i.e., by selecting, for the extrados and intrados of the profile, two flow lines of the family interlinked by a condition impressed on the volume of fluid in the channel constituted by two consecutive blades.

This statement in no way invalidates the general character of the /27
method proposed here for calculation of aerodynamic stresses. We shall see in Chapter 3 that these stresses depend exclusively on the limit conditions at infinity (this is the direct result of application of the Kutta and Joukowski theorem). However, the calculation of aerodynamic moments, through application of the second Blasius formula (ref. 3), depends on limit conditions at finite distance. However, the investigation of the blade vibrations will be limited to bending vibrations, which are highest in the case of relatively short blades, and consequently does not involve the aerodynamic moments.

We should, moreover, add that the correct representation of an existing profile can always be obtained with the aid of not only a single line of vortices, which is too schematic, but by utilizing a rather complex group of vortices and sources arranged along the arcs of identical curves and passing through the points with affix Z_n as in figure 2. At a sufficiently great

TABLE 4.

Identification	$\theta = 260$	$\theta = 270$	$\theta = 280$	$\theta = 290$	$\theta = 310$	$\theta = 320$	$\theta = 330$
r_{n-1}	0,493 (τ)	0,458 (τ)	0,462 (τ)	0,5 (τ)	0,5 (τ)	0,565 (τ)	0,717 (τ)
θ_{n-1}	270°	280°	290°	300°	300°	310°	320°
tg (T_{n-1})	0,9336	0,5267	0,1972	0	0	— 0,1441	— 0,3091
T_{n-1}	43°	28°	11°	0°	0°	— 8°30	— 17°30
$V_{n-1} = T_{n-1} - \theta_{n-1}$	— 227°	— 252°	— 279°	— 300°	— 300°	— 318°30	— 337°30
$d\,\theta_n$	— 10°	— 10°	— 10°	— 10°	10°	10°	5°
$V_{n-1} - d\,\theta_n$	— 217°	— 242°	— 269°	— 290°	— 310°	— 328°30	— 342°30
Sin V_{n-1}	0,7314	0,9511	0,9877	0,8660	0,8660	0,6626	0,3007
Sin ($V_{n-1} - d\,\theta_n$)	0,6018	0,8829	0,9998	0,9397	0,7660	0,5225	0,3827
$r_n = r_{n-1} \frac{\sin V_{n-1}}{\sin (V_{n-1} - d\,\theta_n)}$	0,600 (τ)	0,493 (τ)	0,458 (τ)	0,462 (τ)	0,5650 (τ)	0,717 (τ)	0,912 (τ)
$\lambda_n = \frac{\pi \cdot r_n}{\tau}$		0,493 · π	0,458 · π	0,462 · π	0,565 · π	0,717 · π	
$2\,\lambda_n$		0,986 · π	0,916 · π	0,924 · π	1,130 · π	1,434 · π	
$\theta_n = \theta_{n-1} + d\,\theta_n$		270°	280°	290°	310°	320°	
$\theta_n - \alpha$		150°	160°	170°	190°	200°	
cos ($\theta_n - \alpha$)		0,8660	— 0,9397	— 0,9848	— 0,9848	— 0,9397	
$A_n = 2 \cdot \lambda_n \cdot \cos (\theta_{n-\alpha})$		— 154°	— 155°	— 163°30	— 200°	— 243°	
$a_n = \cos A_n$		— 0,8988	— 0,9063	— 0,9588	— 0,9397	— 0,4712	
$b_n = \sin A_n$		— 0,4384	— 0,4226	— 0,2840	+ 0,3420	0,8910	
sin ($\theta_{n-\alpha}$)		0,5000	0,3420	0,1736	— 0,1736	— 0,3420	
Log $e^{-2\lambda_n \cdot \sin(\theta_n - \alpha)}$		— 1,549	— 0,984	— 0,5040	0,616	1,541	

(Continued)

TABLE 4 (Concluded)

Identification	$\theta = 260$	$\theta = 270$	$\theta = 280$	$\theta = 290$	$\theta = 310$	$\theta = 320$	$\theta = 330$
$h_n = e^{\log h_n}$		0,2125	0,3739	0,6050	1,851	4,668	
$2\,a_n \cdot h_n$		— 0,3820	— 0,6776	— 1,160	— 3,480	— 4,399	
$2 \cdot b_n \cdot h_n$		— 0,1863	— 0,3160	— 0,3440	+ 1,268	8,318	
h_n^2		0,0452	0,1397	0,3660	3,440	21,790	
$1 - h_n^2$		0,9548	0,8603	0,6340	— 2,440	— 20,790	
$\sqrt{3}\,(1 - h_n^2)$		1,6540	1,490	1,098	— 4,225	— 36,010	
$2 \cdot b_n \cdot h_n \cdot + \sqrt{3}\,(1 - h_n^2)$		1,468	1,1740	0,754	— 2,957	— 27,692	
$2 \cdot b_n \cdot h_n \cdot \sqrt{3}$		— 0,3226	— 0,5473	— 0,596	2,195	14,410	
$d_n^1 = 2 \cdot b_n \cdot h_n \cdot \sqrt{3} + h_{n-1}^2$		— 1,2774	— 1,4076	— 1,230	4,635	35,200	
$h_n^2 + 1$		1,0452	1,1397	1,3660	4,440	28,790	
$h_n^2 + 1 - 2\,a_n \cdot h_n$		1,427	1,8173	2,526	7,920	27,189	
$d_n^2 = 2\,(h_n^2 + 1 - 2\,a_n\,h_n)$		2,854	3,6346	5,052	15,840	54,378	
$d_n = d_n^1 + d_n^2$		1,577	2,2270	3,822	20,475	89,578	
$\operatorname{tg} T_n = \frac{2\,b_n \cdot h_n + \sqrt{3}\,(1 - h_n^2)}{d_n}$		0,9336	0,5267	0,1972	— 0,1441	— 0,3091	
T_n		43°	28°	11°	— 8°30	— 17°30	

distance from one of these arcs, we necessarily find an aerodynamic configuration close to that determined by the single line of vortices, because we are finally rather well forced to satisfy the predetermined arrangement of the velocity diagram. Simultaneously, the circulation of the velocity factor taken along a curve enclosing the respective arc within it takes the same value since the sum of the residue in the complex integration corresponding to the first Blasius formula (ref. 3) is the same in both cases.

Specifically, the numerical application given in Section 2 tends to show that for any velocity diagram we can define an ideal profile which constitutes a generalization of all possible profiles of the blade cascades satisfying the same limit conditions. Since we have established a correspondence between all usable velocity diagrams and all type (1) vortical distributions, we can be certain that the results obtained by such distribution apply to all turbines.

The constitution of a profile on the basis of a family of flow lines defined by the potential function (3) is, however, itself affected by uncertainty in regard to the leading and trailing edges of the profiles. The flow lines,

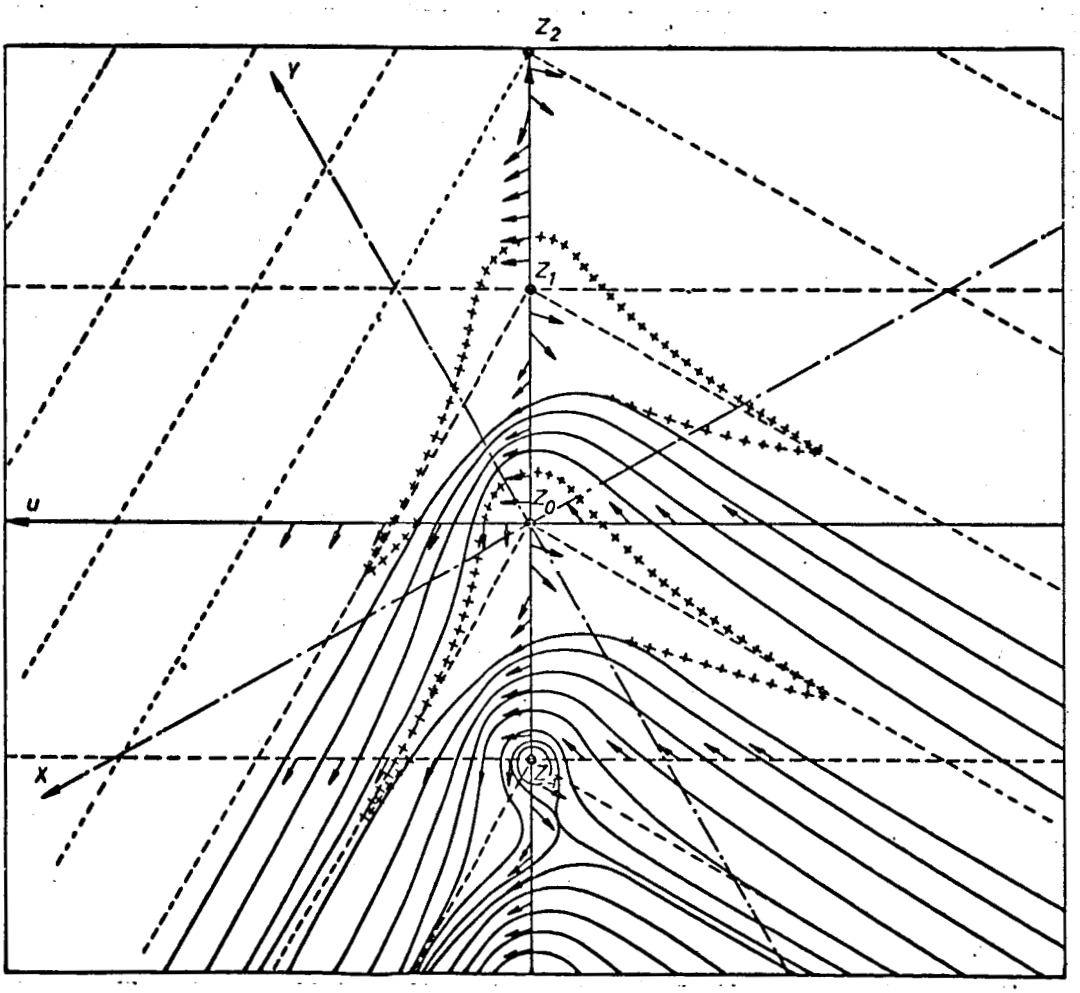

Figure 10

in conformity with the disposition of the velocity diagram, are practically parallel as soon as they deviate slightly from the vortical axis, and we know only within the deviation between the one which serves as intrados and the one which serves as extrados, the upstream point of impact and the downstream profile tip. For the downstream tip, this theoretical imprecision agrees with physical reality because the Kutta-Joukowski condition is never perfectly satisfied and the direction of the velocity at a point of the extrados immediately adjacent to the profile tip always differs in practice by a few degrees from the direction of the tangent to the extrados at this point. These points must be taken at the origin of the wake from each vane of the blading, which wake thickens out at the rate at which, with increase of the Reynolds number, we come closer to the conditions under which turbulence invades the channel constituted by two consecutive vanes. While this transition takes place, the point where aerodynamic velocity ceases to be parallel to the tangent to the extrados rises on the extrados until it becomes stationary at the point where the velocity of potential flow is maximum. It should be understood of course that it will be necessary to take these phenomena into account, during /28 investigation of damping, by means of hypotheses which should be made as simple as possible.

The numerical results in tables 1, 2, 3 and 4 have been plotted in figure 10, which represents the blades of a cascade obtained on the basis of numerical data introduced at the beginning of Section 2. In general, we can always select as intrados the flow line C, which is the flow boundary between two consecutive profiles as it was determined by table 4. The extrados can then be deduced from the datum of flow volume q passing through the channel constituted by two consecutive vanes.

CHAPTER 3. ANALYSIS OF STRESSES APPLIED TO EACH BLADE OF THE RESPECTIVE ROTOR

3.1. Formulation of Aerodynamic Stresses Under Steady-state Regime

These stresses can be deduced from the initial datum of the velocity diagram through application of the Euler theorem. We shall see, however, that analytical integration by the first Blasius formula suggests an extension of the idea of aerodynamic circulation to calculation of the stresses in alternate transient regimes. /29

A. Application of the Euler Theorem

The geometric mean $\overline{W_m}$ of the relative velocities at output and discharge ($\overline{W_1}$ and $\overline{W_2}$) is inclined by angle α to the tangent to the rim at the respective blade base. Aerodynamic stress $\overline{F}$ is broken into a stress normal to the rim $\overline{F_u}$ (thrust on shaft) and a tangential stress $\overline{F_y}$ (motive or resistant) as indicated in figure 11.

$\overline{F_y}$ is obtained by writing the variation of quantity of the tangential motion

$$\overline{F_y} = -S \cdot m_s \cdot \overline{W_{m_u}} (\overline{W_{2_y}} - \overline{W_{1_y}}) = -q \Delta \overline{W}, \tag{13}$$

where s designates the section $\tau \cdot t$ of a channel and $S \cdot m_s \cdot W_{m_u}$ is the flow volume q in this channel.

$\overline{F_u}$ is given by expansion or compression across the blades

$$\overline{u} \cdot \overline{F_u} = s \cdot d_p = S \cdot \frac{1}{2} \cdot m_s \cdot (W_2^2 - W_1^2) = \frac{S \cdot m_s}{2} (\overline{W_2} - \overline{W_1}) (\overline{W_2} + \overline{W_1}),$$

$$\overline{u} \cdot \overline{F_u} = S \cdot m_s (\overline{W_2} - \overline{W_1}) \overline{W_m} = S \cdot m_s (\overline{W_{2_y}} - \overline{W_{1_y}}) \overline{W_{m_y}} + (\overline{W_{2_u}} - \overline{W_{1_u}}) \overline{W_{m_u}},$$

$$\overline{u} \cdot \overline{F_u} = S \cdot m_s (\overline{W_{2_y}} - \overline{W_{1_y}}) \overline{W_{m_y}},$$

since W_{2_u} is equal to W_{1_u} if the fluid is incompressible.

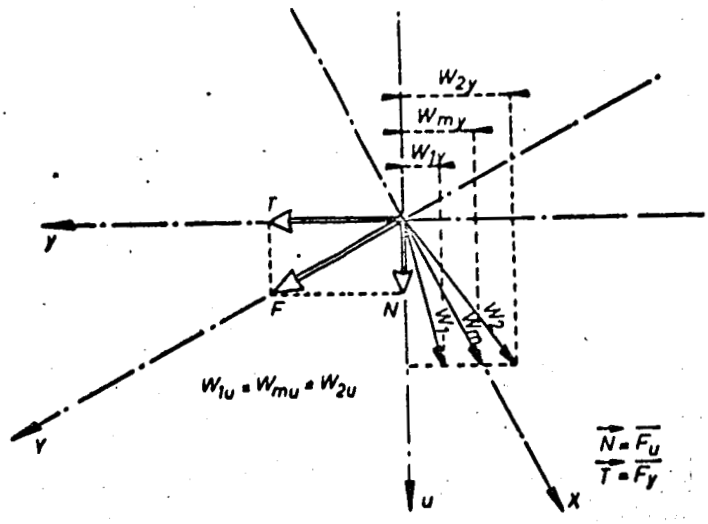

Figure 11

The quotient $\frac{\overline{F_u}}{\overline{F_y}}$ consequently is

$$\frac{\overline{F_u}}{\overline{F_y}} = -\frac{S \cdot m_s \cdot (\overline{W_{z_y}} - \overline{W_{1_y}})\,\overline{W_{m_y}}}{S \cdot m_s \cdot (\overline{W_{z_y}} - \overline{W_{1_y}})\,\overline{W_{m_u}}} = -\frac{\overline{W_{m_y}}}{\overline{W_{m_u}}},$$

which shows that the resultant of the $\overline{F}$ stresses is perpendicular to $\overline{W_m}$. /30
In addition, we have

$$|\overline{F}| = |\overline{W_m}| \cdot \frac{|\overline{F_y}|}{|\overline{W_{m_u}}|},$$

$$|\overline{F}| = S \cdot m_s \cdot |\overline{W_m}| \cdot |\overline{W_{z_y}} - \overline{W_{1_y}}|.$$

B. Application of the First Blasius Formula (ref. 3)

This formula is written

$$\text{Conjugated } (\overline{F}) = \frac{i \cdot m_s \cdot l}{2} \int_{\text{blade}} \left(\frac{d\,\Phi_s}{dz}\right)^2 dz,$$

where integration was made along the blade profile and the blade, e.g., the one located at the origin of the XOY axes, is considered a cylindrical element with length l. However

$$\left(\frac{d\Phi_s}{dz}\right)^2 = W_m^2 - \frac{iW_m \cdot \gamma}{\tau \cdot e^{i\alpha}} \operatorname{cotg} \frac{\pi z}{\tau \cdot e^{i\alpha}} - \frac{\gamma^2}{4 \cdot \tau^2 \cdot e^{2i\alpha}} \operatorname{cotg}^2 \frac{\pi z}{\tau \cdot e^{i\alpha}};$$

on the other hand, in the origin vicinity

$$\operatorname{cotg} \frac{\pi z}{\tau \cdot e^{i\alpha}} = \frac{1}{\frac{\pi z}{\tau \cdot e^{i\alpha}}} - \frac{1}{3} \frac{\pi z}{\tau \cdot e^{i\alpha}} + \varepsilon;$$

the corresponding residue of the term in $\frac{1}{z}$ for $\frac{d\Phi_s}{dz}$ therefore is /31

$$-\frac{W_m \cdot \gamma \cdot i}{\pi},$$

that is

$$\int_{\text{blade}} \left(\frac{d\Phi_s}{dz}\right)^2 dz = -2i\pi \frac{W_m \cdot \gamma \cdot i}{\pi},$$

and then

$$\overline{F} = -i \cdot m_s \cdot 1 \cdot W_m \cdot \gamma = \frac{-i \cdot m_s \cdot S \cdot W_m \cdot \gamma}{\tau}.$$

We again find that the resultant of the aerodynamic stresses $\overline{F}$ is perpendicular to $\overline{W_m}$ which is carried by OX. By projection on Oy we also have

$$m_s \cdot S \cdot W_{m_u} = q$$

and

$$\gamma = \tau \cdot \overline{\Delta W} = \tau (\overline{W_{2_y}} - \overline{W_{1_y}}),$$

from formula (5). Finally the expression of the motive or resistant force is exactly that given by formula (13)

$$\overline{F_y} = -\frac{q\gamma}{\tau} = -S \cdot m_s \cdot W_{m_u} \cdot (\overline{W_{2_y}} - \overline{W_{1_y}}). \qquad (13A)$$

However, it may be objected that interpretation of the profile lift through the theory of circulation of the velocity vector is valid only in the incompressible field. The subsonic range is sufficiently important to remain within it by introducing, as a first approximation, the phenomena of compressibility in the form of correcting factors in $\sqrt{1 - M^2}$, where M designates the Mach number; then we have

$$\gamma = -\frac{\tau \cdot W_1}{\sqrt{1 - M^2}} \cdot \frac{\sin \psi}{\cos (\psi - m)}. \qquad (5A)$$

Transposition of the expression for circulation from the field of incompressible flow to the field of compressible flow is thus modeled on the transposition proposed by Prandtl, Glauert and Ackeret for C_z. Accordingly,

conditions for strict application of formula (5A) are that the profiles must be thin and their curvature and incidence slight.

To define the M number, we may call on the fact that linearization of the fluid mechanics equations requires referencing ourselves to an overall flow velocity and expressing this velocity at any point using perturbations considered infinitely small and where we neglect their square. It is consequently convenient to select, for the M number, the ratio of the geometric mean velocity relative to the speed of sound a_m at those points where this velocity W_m

is attained in the respective incompressible flow defined by relations

$$\begin{cases} (h_0^2 - 1)\cos\alpha - 2h_0 b_0 \sin\alpha = 0, \\ 2h_0 b_0 \cos\alpha + (h_0^2 - 1)\sin\alpha = 0. \end{cases}$$

More precisely, if we develop the complex potential Φ of equation (1) /32 in the form

$$\Phi = \Phi_R(x, y) + i\,\Phi_I(x, y),$$

the general equation to which the potential Φ_R is subject in the xOy axes

is written, employing the notation customary for the laplacian and by designating the speed of sound by $a_s(x, y)$, as

$$\Delta\Phi_R = \frac{1}{a_s^2}\left\{\left(\frac{\partial\Phi_R}{\partial x}\right)^2\frac{\partial^2\Phi_R}{\partial x^2} + \left(\frac{\partial\Phi_R}{\partial y}\right)^2\frac{\partial^2\Phi_R}{\partial y^2} + 2\frac{\partial\Phi_R}{\partial x}\frac{\partial\Phi_R}{\partial y}\cdot\frac{\partial^2\Phi_R}{\partial x\,\partial y}\right\}.$$

After linearization, this equation becomes

$$\frac{\partial^2\Phi_R}{\partial x^2}\left(1 - \frac{W_m^2}{a_m^2}\right) + \frac{\partial^2\Phi_R}{\partial y^2} = 0,$$

from which results the analogy with incompressible flow in coordinates $\left(\frac{X, Y}{\sqrt{1 - M^2}}\right)$;

The Blasius integration gives the stated result (refs. 11, 24) and the value of a_m results from the datum of upstream temperature (we do know that the variation is in the order of 5° between the terminal point and the points where the velocity reaches 100 m/sec). It should of course be understood that the

specific mass of the equivalent incompressible fluid is that determined by the conditions of temperature and pressure at the points defined by the above relations, where the temperature is taken as equal to the temperature of the upstream flow.

For the numerical application given in Section 3 of Chapter 2, the order of magnitude of the respective perturbation is given by the ratio

$$\frac{W_{2y}}{W_m} = \sin \alpha = 0.5$$

and therefore we cannot expect to derive the aerodynamic stresses from formula (5A) with a precision greater than 25 percent, when the Mach number approaches 1. It is true that the curvature of the investigated profile is particularly pronounced.

3.2 Significance of Formulas Obtained for Aerodynamic Stresses Under Steady Regimes

Both formulas in $q\overline{\Delta W}$ and $\frac{q\gamma}{\tau}$ (13) and (13A) stress the fact that the blades of the same rim may be charged unequally if the total volume across the rotor is not uniformly distributed between the channels. However, the formula in $q\overline{\Delta W}$ states only the existence of a tangential variation of the quantity of motion, whereas the formula in $\frac{q\gamma}{\tau}$ also specifies this variation of the quantity of motion or, in other words, this conversion of the fluid's usable energy into mechanical energy (ref. 7) is linked to the nonuniformity of the potential function describing the flow. (For this reason we prefer to /33 introduce compressibility by affecting it with the coefficient $\frac{1}{\sqrt{1-M^2}}$ rather than to employ, as is customary, the arithmetic mean between the specific mass upstream and downstream, which would have complicated the expression of the aerodynamic stresses as a function of time.)

Of particular importance is the application to formula (13A) of the Lagrange theorem according to which "if a fluid is set in motion, all its possible motion takes place with uniform potentials of velocity."

Since the cascade upstream flow may be considered as having uniform velocity we actually will not be able, assuming the fluid to be perfect, to produce at the level of the cascade, vortices perpendicular to the plane of flow anymore than in the case of a plane wing whose behavior is not fundamentally different from that of a cascade, and utilization of a nonuniform potential function of type (1) would merely serve to artificially create the paradox of d'Alembert-Cisotti (ref. 4). Some authors (ref. 20) consider that

if the resultant of the aerodynamic stresses applied to a simply connected body having three finite dimensions is zero for uniform upstream flow, in return, the paradox can no longer be sustained in the case of an indefinitely elongated cylinder. Nevertheless, in this study we shall assume that a torus of finite dimensions is not exempt from the paradox of d'Alembert-Cisotti (which can be demonstrated) and (but without demonstration) that passage to the limit of the torus to the cylinder does not introduce discontinuity in the function

$$C_p = \frac{F_p}{\frac{1}{2} p S V_0^2},$$

defined as the ratio of the projection on the axis of the torus of the aerodynamic resultant to the product, by the dynamic pressure in the uniform upstream flow, of the surface of the apparent contour of the object for an observer at infinity in the selected direction (ref. 12).

We therefore consider that only viscous fluids are able to indefinitely and stably support objects heavier than they, where the vortices necessary for calculating stresses by the Prandtl method for plane wings (refs. 12, 26) and by formula (13A) are produced permanently within the limit curve as outlined in reference 47 for the Oseen equations. Each term in $L(z - in\tau e^{i\alpha})$ of formula (1) constitutes, under this concept, a type of mathematical integration summing the nonuniform potentials of very small elementary intensity linked to all the vortices existing in the boundary layer adhering to the profile. The concepts of boundary layer, circulation and Reynolds number, where the latter allows us to simply introduce the fluid viscosity into the formulas, therefore play a fundamental role in all the following.

For profiles designed other than according to the considerations developed in Section 3 of Chapter 2, it is possible to schematize the behavior of any blading with greater exactitude by breaking down each term in $n\tau e^{i\alpha}$ into elements localized on a curve arc passing through the affix point $in\tau e^{i\alpha}$. The result of the integration contained in the first Blasius formula is the same, but the pressure center is displaced and the aerodynamic moment, calculated with the second Blasius formula /34

$$M_0 = -\frac{m_s \cdot l}{2} \text{ real part } \left\{ \left(\frac{d\Phi_s}{dz} \right)^2 z\, dz \right\},$$

depends on the breakdown mode adopted.

It should be understood, of course, that production of the vortices is a component of the energy balance. In the viewpoint adopted, we regard the expression of profile losses as a particular form given to that of the yield from conversion of usable energy into mechanical energy absorbed or transmitted

by the machine shaft. Their amount may vary when part of the usable energy serves either to damp vibrations (positive damping) or to emphasize them (negative damping).

We can compare the proposed analysis to that by Prandtl (ref. 24) in his theory for permanent motion of a fluid around a wing of limited span. Formula (5A) retains only the influence of the linked vortices parallel to the span which helped him to give the expression of the lift for infinite span perpendicular to the general direction of flow. Neglecting the free vortices, it does not consider the induced drag which appears with introduction of the limited span concept, i.e., a reduction of local incidence equal to the quotient of the perturbating velocity due to the free vortices by the overall velocity of the flow W_m. Because the Prandtl induced polars are parabolas, simplification consists in assimilating them to their tangent at the apex. We thus specify the limits of application of the proposed hypothesis in order to justify development of a circular cascade along a plane and ultimately to eliminate the possibility of torsional vibration.

On the basis of the preceding remarks of a physical order, we have attempted below to establish the necessary relations between investigation of the blades under steady-state regime and under alternate transient regime.

3.3 Formulation of Aerodynamic Stresses Under Alternate Transient Regime

A. Circulation Oscillations

If we assume that the flow volume q in a channel is strictly constant, formula (13A) shows that the stress $\overline{F_y}$ may still vary as the circulation γ which appears in the form of a function of angle ψ in formula (5A)

$$\gamma = -\frac{t \cdot W_1}{\sqrt{1-M^2}} \cdot \frac{\sin \psi}{\cos(\psi - m)}.$$

However, during alternating vibration precisely the angle ψ assumes an increase $d\psi$ as shown in figure 12. It is therefore possible to calculate by ψ the circulation oscillations as a function of time and to deduce from this /35 the second number of the equation for vibrations.

Let $(y_p)_M$ actually be the pseudo-amplitude of vibration at a given instant counted in relation to the xyu axes linked to the rotor. A fluid particle arriving at D which would have been at C after having followed the extrados in continuous aerodynamic regime is in fact situated at J at the blading exit, provided there has been no detachment at the profile tip. Utilizing the notations in figure 12, we can write

and then

$$\overline{GJ} = -dy,$$

$$d\psi = \frac{\overline{GH}}{\overline{DG}} = -\frac{dy \cdot \cos\theta_1}{\frac{e}{\cos\theta_1}} = -\frac{dy \cdot \cos^2\theta_1}{e}$$

where e designates the blading depth and θ_1 the profile chord inclination in relation to the turbine axis, from which we deduce

$$d\gamma = \frac{d\gamma}{d\psi} d\psi = -\frac{\tau \cdot W_1 \cos m}{\sqrt{1 - M^2 \cos^2(\psi - m)}} \left\{ -\frac{dy \cdot \cos^2\theta_1}{e} \right\}. \qquad (14)$$

In the absence of detachment, evaluation of dy results from figure 12 as

$$dy = (y_p)_M \{ \sin\omega(t + td) - \sin\omega t \}$$

provided we now assume that elongation y is the product of the sinusoidal function of time whose frequency is not necessarily equal to the natural frequency of the blades constituting the respective cascade, and of the pseudo-amplitude $(y_p)_M$ slowly varying in time.

A first consequence of this formulation is that damping may now be defined as negative, positive or zero, depending on whether the pseudo-amplitude is a function of time respectively decreasing, increasing or quasi-constant.

In addition, however, the result of such a formula is that, considering in practice the brief interval t_d in which the blading is traversed by /36

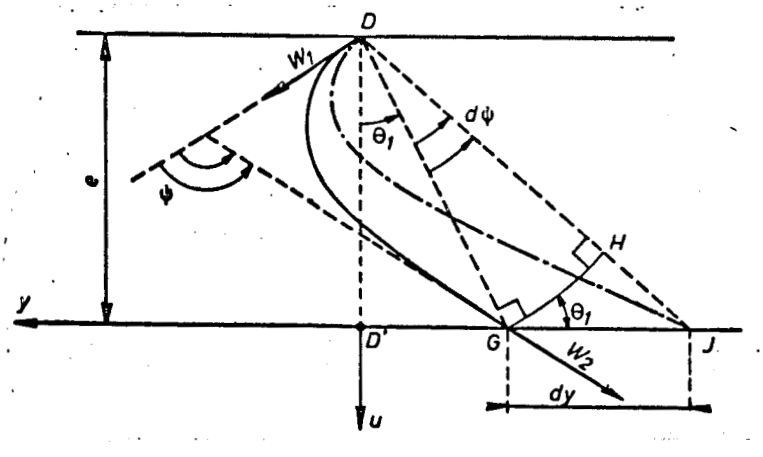

Figure 12

the fluid compared to the oscillation period, the deviation of dγ is almost in square with the elongation y, hence its importance in regard to damping. This passage interval t_d

$$t_d = \frac{c_d}{W_m}$$

may be defined as the quotient of the profile chord c_d by the mean velocity such as it appears in figures 2, 6 and 8 (neglecting the oscillation of t_d concomitant with that of y).

We subsequently introduce the idea of detachment at the profile tip with a more complete expression of dy

$$dy = \left\{ (y_p)_M - \frac{c_d |\psi|}{\cos \theta_1} \cdot d_p (\mathrm{Re}) \right\} \left\{ \sin \omega (t + t_d) - \sin \omega t \right\}. \qquad (15)$$

The importance of this mathematical pattern in all that follows and, of course, in the study conclusions themselves, necessitates explanation of its constituting terms: dy is the elongation variation controlled by variation of the aerodynamic stresses during evolution of the velocity diagram. This variation is reduced by the detachments at the profile tip in accordance with figures 12-1, 12-2, 12-3.

(1) In steady-state regimes, a fluid particle arriving at D and not "adhering" to the profile DG would leave the blading at G'_1, such that

$$G'_1 G = \frac{GH}{\sin \left\{ \frac{\pi}{2} - (\theta_1 + \psi) \right\}} \# \frac{GH}{\cos \theta_1} = \frac{c_d \cdot |\psi|}{\cos \theta_1}$$

within the second order when the angle ψ is itself an infinitesimal of the first order (fig. 12-1).

(2) In steady-state regimes, a particle arriving at D actually becomes detached (fig. 12-2) only at a slight distance a_d from the profile tip DG and leaves the blading at G'_2, such that

$$GG'_2 = \frac{GH}{\cos \theta_1} = \frac{a_d \cdot e_p}{\cos \theta_1}.$$

We can assume that GG'_2 differs from GG'_1 only by a factor $d_p(\mathrm{Re})$ characterizing the importance of the phenomena linked to the fluid velocity and viscosity and to the blading geometry

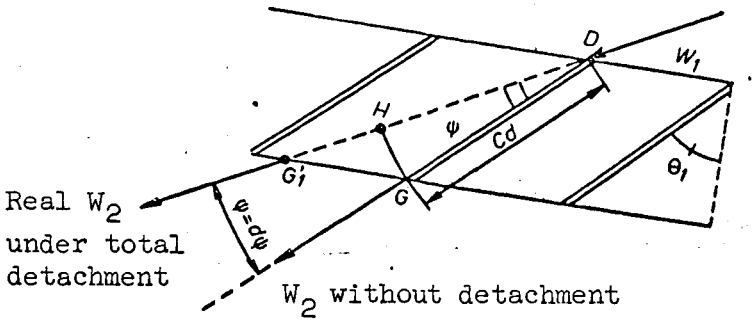

Figure 12-1

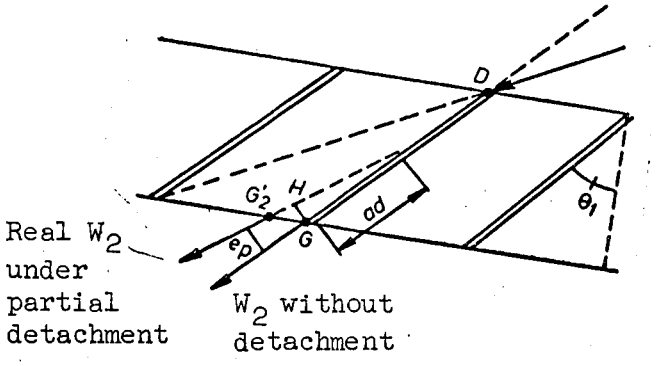

Figure 12-2

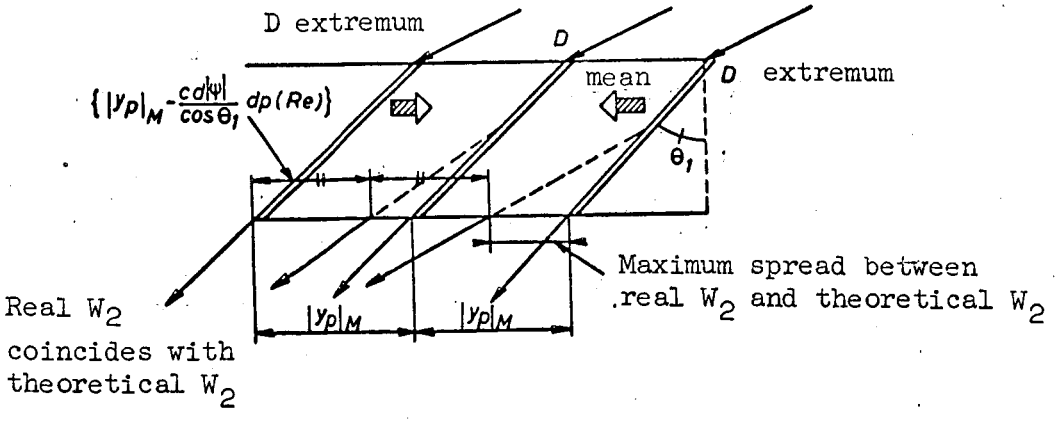

Figure 12-3

$$GG'_2 = GG'_1 \cdot d_p\,(\mathrm{Re})$$

or also

$$\underline{a_d \cdot e_p = c_d \cdot |\psi| \cdot d_p\,(\mathrm{Re}),} \qquad (15')$$

This last equation must be interpreted as follows:

(a) at constant flow velocity and, more generally, with constant Reynolds number, any variation of ψ is translated by a proportional variation of e_p if the distance of the detachment point from the profile tip has not varied;

(b) e_p may be considerable at very slight incidence, provided the detachment manifests itself in the immediate proximity of the profile tip, and may be invariant when ψ varies if the detachment point deviates from the profile. However, at very slight incidence, the proportionality with ψ will probably be obscured by the occurrence of detachments independent of the incidence whose origin must be sought in the geometry of the profile. /38

In a vibratory regime, the blade's oscillating motion has both the tendency to reattach the flow lines detached in steady-state regimes and to aggravate this detachment in such manner that the double amplitude of the fluid oscillation is less than the double amplitude of blade oscillation (fig. 12-3). This phenomenon can therefore be taken into account at least approximately, and especially the local accelerations in the fluid at the points for which the blade velocity is zero, assuming that there is complete cancellation of detachment when elongation is equal to the pseudo-amplitude and directed opposite to the fluid deviation. Since the fluid oscillation mid-point must necessarily be the point G'_2 identified under continuous flow (fig. 12-2), the pseudo-amplitude of fluid elongation then appears equal to

$$(y_p)_M = \frac{c_d \cdot |\psi|}{\cos\theta_1} \cdot d_p\,(\mathrm{Re}).$$

Conditions for applying formula (15) therefore are as follows:

a. Selection of Reynolds number Re

Re should characterize local equilibrium between the fluid's inertial forces and the viscosity forces determining adhesion of the fluid to the profile and characterize also the blading geometry.

We can use at least two very classical forms given to the Reynolds number:

$$(\mathrm{Re})_{\text{profile}} = \frac{W_m \cdot c_d}{\nu},$$

$$(\mathrm{Re})_{\text{channel}} = \frac{W_m \cdot D_h}{\nu},$$

in which ν is the kinematic viscosity of the fluid and D_h is the hydraulic diameter

$$D_h = \frac{4 \cdot \text{line segment}}{\text{contact perimeter}} = \frac{4 \cdot l \cdot \tau \cdot \cos \theta_1}{2\,(l + \tau \cos \theta)_1};$$

Moreover, there is a relation between the two

$$\mathrm{Re}_{\text{channel}} = \frac{2 \cdot c_d \cdot W_m}{\nu} \cdot \frac{\frac{l}{c_d} \cdot \frac{\tau}{c_d} \cdot \cos \theta_1}{\left\{ \frac{l}{c_d} + \frac{\tau}{c_d} \cdot \cos \theta_1 \right\}},$$

that is

$$\mathrm{Re}_{\text{channel}} = 2 \cdot \mathrm{Re}_{\text{profile}} \cdot \text{function (elongation, relative pitch, setting)}.$$

In both cases we use again the concept of circulation /39

$$2 \cdot \mathrm{Re}_{\text{profile}} \cdot \nu = 2 \cdot c_d \cdot W_m \# \frac{c_d}{\tau} \cdot \gamma$$

(cf. Section 3, Chapter 2), but the Reynolds number which is introducing the hydraulic diameter is the most significative and should be preferred over the other because it allows taking into account the pitch effect.

b. Influence of span

Here again we neglect to differentiate the flow sections from the aerodynamic viewpoint and do not take into account the ends effects, except through elongation and relative pitch. Formula (15) is therefore applied to the profile median section and is subsequently compensated for by calculation to satisfy the limiting conditions of the mechanical problem (cf. Section 1, Chapter 4).

c. Determination of the function $d_p(\mathrm{Re})$

To determine this as defined above, we make wind-tunnel measurements allowing us to determine, under nonvibratory operation, the deviation between the value ψ resulting from study of the theoretical velocity diagram and the value of the angle formed by the real relative velocities of fluid intake and discharge from the blading. We can also localize the detachment point on the profile whose example is given in Chapter 6.

Finally, the circulation oscillations can be expressed as follows

$$\gamma = \gamma_0 + d\gamma = \gamma_0 + \frac{d\gamma}{d\psi} d\psi = \gamma_0 + \gamma_1 \sin(\omega t + j)$$

with

$$\gamma_1 \cdot \sin(\omega t + j) = \frac{\tau \cdot W_1 \cdot \cos m}{\sqrt{1 - M^2 \cos^2(\psi - m)}} \cdot \frac{\cos^2 \theta_1}{e} \cdot \left\{ (y_p)_M - \frac{c_d |\psi|}{\cos \theta_1} \cdot d_p (\mathrm{Re}) \right\} C_r$$

and

$$C_r = \sin \omega t_d \cdot \cos \omega t - 2 \sin^2 \frac{\omega t_d}{2} \cdot \sin \omega t,$$

or

$$\gamma_1 \cdot \sin(\omega t + j) = \gamma_1 \{ \sin \omega t \cdot \cos j + \cos \omega t \cdot \sin j \},$$

$$\mathrm{tg}\, j = -\operatorname{cotg} \frac{\omega t_d}{2},$$

$$j = -\frac{\pi}{2} + \frac{\omega t_d}{2}, \tag{15A}$$

$$\gamma_1 = -\frac{2 \cdot \tau \cdot W_1 \cos m}{\sqrt{1 - M^2} \cdot e} \cdot \frac{\cos^2 \theta_1}{\cos^2(\psi - m)} \cdot \sin \frac{\omega t d}{2} \left\{ (y_p)_M - \frac{c_d |\psi|}{\cos \theta_1} \cdot d_p (\mathrm{Re}) \right\}. \tag{15B}$$

The formulas thus obtained will be discussed during investigation of actual damping in Chapter 5. However, it is interesting to note even now that it will be convenient, as we continue calculation, to break down $(\gamma)_1 \sin(\omega t + j)$ into /40

$$\left\{ + \frac{\tau \cdot W_1 \cdot \cos m}{\sqrt{1 - M^2} \cdot e} \cdot \frac{\cos^2 \theta_1}{\cos^2(\psi - m)} \right\} \frac{1}{\omega} \sin \omega t_d \frac{dy_p}{dt} - 2 \sin^2 \frac{\omega t_d}{2} y_p \Bigg\}$$

$$\left(- \frac{\tau \cdot W_1 \cos m}{\sqrt{1 - M^2} \cdot e} \cdot \frac{\cos^2 \theta_1}{\cos^2(\psi - m)} \cdot \frac{c_d |\psi| \cdot d_p (\mathrm{Re})}{\cos \theta_1} \cdot 2 \sin \frac{\omega t d}{2} \cos \omega \left(t + \frac{t_d}{2} \right) \right.$$

neglecting the assumed slow variation of $(y_p)_M$, i.e., supposing that the derivative $\frac{d}{dt} (y_p)_M$ is very slight.

d. Local volume oscillations

For volume oscillations in the channel constituted by two consecutive vanes, formula (13A) furnishes an additional stress

$$dF_y = -\frac{\gamma}{\tau} \cdot d_q,$$

where

$$d_q = d(m_s \cdot S \cdot W_{m_u}) = m_s \cdot W_{m_u} \cdot l \cdot \left(\frac{y_p - y_{p-1}}{2} + \frac{y_{p+1} - y_p}{2} \right),$$

and, for each blade, y_p designates the distance from the midpoint to a radial axis Ox_p passing through the blade base.

The consequences of this local volume oscillation can be investigated by an equivalent formula in $m_s(W_{m_u}(y_p - y_{p-1}))$ if we adopt for y_p the form

$$y_p = y_0 \cdot \sin\left\{\cot - \frac{2(p-1)\pi}{N_0}\right\};$$

Actually, the difference between $\frac{y_{p+1} - y_{p-1}}{2}$ and $y_p - y_{p-1}$ is expressed by

$$\frac{\sin\left\{\omega t \frac{2p}{N_0}\pi\right\} + \sin\left\{\omega t - \frac{2(p-2)\pi}{N_0}\right\}}{2} - \sin\left\{\omega t - \frac{2(p-1)\pi}{N_0}\right\}$$
$$= \left(\sin\left\{\omega t - \frac{2(p-1)\pi}{N_0}\right\}\right)\left(\cos\left\{\frac{\pi}{N_0}\right\} - 1\right)$$

and it is sufficient that N_0 is greater than 7 so that this term will be negligible within 10 percent. We therefore take

$$dF_y = -\left|\gamma_0 + \gamma_1 \sin \omega t\right| \cdot m_s \cdot l \cdot W_{m_u} \cdot \frac{y_p - y_{p-1}}{\tau} = F_y \cdot \frac{y_p - y_{p-1}}{\tau}. \qquad (16)$$

Chapter 4 discusses specifically the details for applying formula (16). /41 The conditions under which the subject of influence of the free vortices has been neglected throughout this section should again be specified from different viewpoints:

-- First, in regard to the absence of detachment. Circulation variation in a nondetached regime generates damping and is inevitably expressed by emission, strictly at the profile tip, of free vortices parallel to the span. These vortices, if they were generated in a nonviscous fluid by some process, would modify the lift, which is calculated on the basis of the linked vortices, and also the aerodynamic moment. In viscous fluid, these vortices have little influence, because the rotational energy they contain is rapidly dissipated into heat, specifically in the case of bending vibrations, for which the damping effect resulting from relation (14) is due to a variation of ψ (or incidence, see Chapter 6, figs. 16 and 17). However, for torsional vibrations, the incidence variations may have no influence on the aerodynamic moment if the mechanical axis of torsion runs sufficiently close to the center. We must then introduce the "installation function" for lift calculated by Wagner (ref. 23), since the orders of magnitude are sufficiently low to be compared with those of internal damping of the blade material.

-- Second, in regard to detachment. We specify further (Chapter 5) how on the extrados the rise of the origin of the free vortices, which introduces fluctuations into the geometry of the velocity diagram, causes cancellation of the damping originating these vortices in the absence of detachment. On the experimental plane, the distinction between alternate vortices resulting from circulation oscillation and vortices released in a detached regime is perfectly clear, since the detachment can be observed in the absence of vibrations (e.g., aircraft stalling).

In the final analysis we thus find that it is entrance of vortices pre-existing under a detached regime into an oscillating regime which provokes the instability, whether this concerns an isolated profile or a cascade (except for some differences discussed at the end of Chapter 4). It is probable that no fatigue rupture has ever been observed on isolated profiles vibrating under flexure. However, the existence of instability through detachment is evident at least in the relaxation oscillations of a flag because the wing loads of isolated profiles are too slight to present any danger of fatigue. Certain precise facts determined in regard to cascade profiles operating at high temperatures (first stage of steam turbines) (ref. 13) confirm this viewpoint.

Finally we should add that the preceding reasoning was developed by taking the resultant of the aerodynamic stresses, implicitly assumed as uniformly distributed, in the center of the blade axis. To conserve the general character of the exposé, we shall consider in the following, whenever necessary, that the aerodynamic stress $(F_y + dF_y) \cdot \frac{dl}{l}$ is applied to an element of the blade axis with length dl in the center of this element.

3.4 Elastic, Inertial and Centrifugal Stresses

We do not investigate the case of blades joined at the top because one /42
of the study's objectives is precisely to provide a better knowledge of the vibratory phenomena so as to avoid recourse to devices which inhibit these phenomena and reduce yield.

The blade is considered as a relatively short, flexible knife blade with torsional deformations consequently negligible in comparison to bending deformations. This blade is implanted at the origin of the xyu axes along Ox, and its mass P is assumed to be concentrated in as many points, equidistant from the blade axis and taken as an odd number, as is necessary to attain the desired precision in evaluating the mechanical stresses (ref. 23).

Figure 13 represents the breakdown into three punctiform masses. By following this simple example and temporarily disregarding the centrifugal forces, we shall show how a complete calculation should be carried out if we desire anything other than an analytical explanation of the phenomena of vibratory damping in the turbine blading. The figure shows that the elastic line is broken into four sections in accordance with the four differential equations

$$
\left.
\begin{aligned}
EI\,y''_1 &= \left(-\frac{P}{3}\frac{d^2 Y_1}{dl^2} + \frac{F_y}{3}\right)\left(\frac{l}{6} - x\right) \qquad (1)\\
&+ \left(-\frac{P}{3}\frac{d^2 Y_2}{dl^2} + \frac{F_y}{3}\right)\left(\frac{3\,l}{6} - x\right)\\
&+ \left(-\frac{P}{3}\frac{d^2 Y_3}{dl^2} + \frac{F_y}{3}\right)\left(\frac{5\,l}{6} - x\right);\\
EI\,y''_2 &= \left(-\frac{P}{3}\frac{d^2 Y_2}{dl^2} + \frac{F_y}{3}\right)\left(\frac{3\,l}{6} - x\right) \qquad (2)\\
&+ \left(-\frac{P}{3}\frac{d^2 Y_3}{dl^2} + \frac{F_y}{3}\right)\left(\frac{5\,l}{6} - x\right);\\
EI\,y''_3 &= \left(-\frac{P}{3}\frac{d^2 Y_3}{dl^2} + \frac{F_y}{3}\right)\left(\frac{5\,l}{6} - x\right); \qquad (3)\\
EI\,y''_4 &= 0; \qquad (4)
\end{aligned}
\right\} \qquad (17)
$$

(For convenience in calculation, this section assumes that F_y is independent of time. In the contrary case, the pendular equations (19) are replaced by equations that all have the same second member $F_y/3$. Investigation of the elastic deformation of a blade is made in the same manner. In addition, the aerodynamic damping forces are small in relation to the other stresses applied to the elastic line, so that the results obtained in this section and pertaining to natural frequencies and maximal values of the elastic stresses are independent of the results obtained for vibratory damping in Chapter 5.)

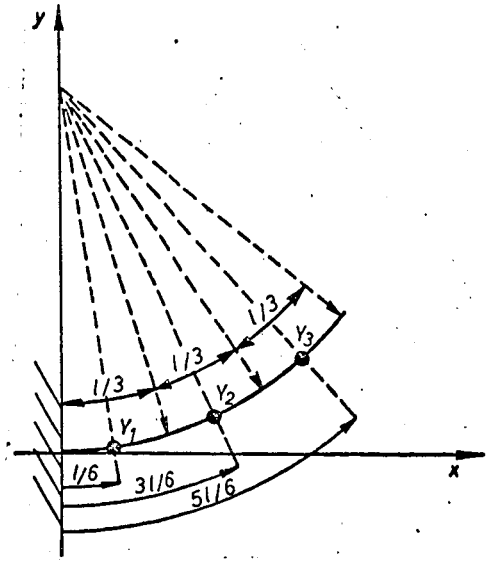

Figure 13

For equation $(17)_4$ we desire a solution of the form /43

$$F_4 = f_4(x)\, h(t) \tag{18}$$

and we have $$y''_4 = f''_{4x}(x) \cdot h(t) = 0, \quad \text{i.e.,} \quad f''_{4x} = 0$$

$$f_4(x) = f'_0 \cdot x + f_0,$$

where f_0 designates the initial amplitude of point Y_3 in figure 13; f'_0, which defines the blade inclination on Ox, results from f_0 and will be furnished as the result of calculation; h(t) is a sinusoidal function at its maximum at the instant zero and consequently must be taken equal to 1 at that instant, but this maximum may vary between values greater or less than 1 during vibration if damping occurs, depending on whether this damping is negative or positive.

We also desire for equation $(17)_3$ a solution of the form

$$y_3 = f_3(x)\, h(t)$$

and we have

$$y''_3 = f''_{3x} \cdot h(t), \quad \text{i.e.,} \quad \begin{cases} y_3 = f_3\left(\frac{5\,l}{6}\right) \cdot h(t), \\ \frac{d^2 y_3}{dt^2} = f_3\left(\frac{5\,l}{6}\right) \cdot h''(t), \end{cases}$$

and further

$$EIf''_{3x} \cdot h(t) = \left\{-\frac{P}{3} \cdot f_3\left(\frac{5\,l}{6}\right) \cdot h''(t) - \frac{F_y}{3}\right\}\left(\frac{5\,l}{6} - x\right).$$

The separation of the variables assumed at the beginning consequently /44 presupposes

$$-\frac{P}{3} \cdot f_3\left(\frac{5\,l}{6}\right) \cdot h''(t) + \frac{F_y}{3} = K_3\, h(t),$$

which, within the constant term, leads to the pendular equation

$$\frac{P}{3} \cdot h'' + \frac{K_3}{f_3\left(\frac{5\,l}{6}\right)} \cdot h = 0. \tag{19a}$$

Subsequently, we deduce the third section equation from

$$EI \cdot f''_{3x'}(x) = K_3 \cdot \left(\frac{5\,l}{6} - x\right).$$

where the integration limit conditions are

$$\begin{cases} \frac{dy_3}{dx}\left(\frac{5\,l}{6}\right) = \frac{dy_4}{dx}\left(\frac{5\,l}{6}\right) \\ y_3\left(\frac{5\,l}{6}\right) = y_4\left(\frac{5\,l}{6}\right) \end{cases} \text{ or } \begin{cases} f'_3\left(\frac{5\,l}{6}\right) = f'_0, \\ f_3\left(\frac{5\,l}{6}\right) = \frac{5\,l}{6} f'_0 - f_0. \end{cases}$$

In the case of equation $(17)_2$ we successively have

$$\frac{P}{3} \cdot h'' + \frac{K_2}{f_2\left(\frac{3\,l}{6}\right)} \cdot h = 0, \tag{19b}$$

$$EI \cdot f''_{2x'} = K_2\left(\frac{3\,l}{6} - x\right) + K_3 \cdot \left(\frac{5\,l}{6} - x\right),$$

with the new limit conditions of the integration

$$\begin{cases} \frac{dy_2}{dx}\left(\frac{3\,l}{6}\right) = \frac{dy_3}{dx}\left(\frac{3\,l}{6}\right) \\ y_2\left(\frac{3\,l}{6}\right) = y_3\left(\frac{3\,l}{6}\right) \end{cases} \text{ or } \begin{cases} f'_2\left(\frac{3\,l}{6}\right) = f'_3\left(\frac{3\,l}{6}\right), \\ f_2\left(\frac{3\,l}{6}\right) = f_3\left(\frac{3\,l}{6}\right). \end{cases}$$

For equation $(17)_1$ we finally have

$$\frac{P}{3} \cdot h'' + \frac{K_1}{f_1\left(\frac{l}{6}\right)} \cdot h = 0 \tag{19c}$$

with the limit conditions at the recess supporting the blade base

$$\begin{cases} \frac{dy_1}{dx}(0) = 0 \\ y_1(0) = 0 \end{cases} \text{ or } \begin{cases} f'_1(0) = 0, \\ f_1(0) = 0. \end{cases}$$

The three constants K_3, K_2, K_1 which appear in the pendular equation /45 are linked by the relations expressing the uniqueness of the three forms obtained and make it possible to assign it a unique number, or (19),

$$\frac{K_1}{f_1\left(\frac{l}{6}\right)} = \frac{K_2}{f_2\left(\frac{3l}{6}\right)} = \frac{K_3}{f_3\left(\frac{5l}{6}\right)}.$$

The denominators may be expressed as a function of the magnitudes f_0 and f'_0 introduced for the first section. To obtain these expressions, it is sufficient to integrate:

(a) in the case of f''_{3x},

$$EI \cdot f'_3 = -\frac{K_3}{2} \cdot \left(\frac{5l}{6} - x\right)^2 + EI \cdot f'_0,$$

hence

$$f'_3 = f'_0 - \frac{K_3}{2EI} \cdot \left(\frac{5l}{6} - x\right)^2$$

and

$$f_3 = f'_0 x + f_0 + \frac{K_3}{6EI} \cdot \left(\frac{5l}{6} - x\right)^2;$$

(b) in the case of f''_{2x},

$$EI \cdot f'_2 = -\frac{K_2}{2} \cdot \left(\frac{3l}{6} - x\right)^2 - \frac{K_3}{2} \cdot \left(\frac{5l}{6} - x\right)^2 + Cte$$

where the constant is determined by the following condition stated above

$$f'_2\left(\frac{3l}{6}\right) = f'_3\left(\frac{3l}{6}\right),$$

taking into account the relation obtained previously

$$EI \cdot f'_3\left(\frac{3l}{6}\right) = EI \cdot f'_0 - \frac{K_3}{2} \cdot \left(\frac{5l}{6} - \frac{3l}{6}\right)^2,$$

hence

$$f'_2 = f'_0 - \frac{K_2}{2EI} \cdot \left(\frac{3l}{6} - x\right)^2 - \frac{K_3}{2EI} \cdot \left(\frac{5l}{6} - x\right)^2,$$

and then

$$f_2 = f'_0 x + f_0 + \frac{K_2}{6EI}\cdot\left(\frac{3l}{6}-x\right)^3 + \frac{K_3}{6EI}\left(\frac{5l}{6}-x\right)^3 + \text{Cte}$$

or, taking into account the equation

$$f_2\left(\frac{3l}{6}\right) = f_3\left(\frac{3l}{6}\right),$$

$$f_3 = f'_0 x + f_0 + \frac{K_2}{6EI}\left(\frac{3l}{6}-x\right)^3 + \frac{K_3}{6EI}\left(\frac{5l}{6}-x\right)^3;$$

(c) in the case of f''_{1_x}, and by analogy with the results obtained /46

$$f'_1 = f'_0 - \frac{K_1}{2EI}\cdot\left(\frac{l}{6}-x\right)^2 - \frac{K_2}{2EI}\cdot\left(\frac{3l}{6}-x\right)^2 - \frac{K_3}{2EI}\cdot\left(\frac{5l}{6}-x\right)^2,$$

$$f_1 = f'_0 x + f_0 + \frac{K_1}{6EI}\cdot\left(\frac{l}{6}-x\right)^3 + \frac{K_2}{6EI}\cdot\left(\frac{3l}{6}-x\right)^3 + \frac{K_3}{6EI}\cdot\left(\frac{5l}{6}-x\right)^3.$$

The denominators of the fractions in K_1, K_2, K_3 therefore are

$$f_3\left(\frac{5l}{6}\right) = \frac{5l}{6}f'_0 + f_0,$$

$$f_2\left(\frac{3l}{6}\right) = \frac{3l}{6}f'_0 + f_0 + \frac{K_3}{6EI}\cdot\left(\frac{2l}{6}\right)^3,$$

$$f_1\left(\frac{l}{6}\right) = \frac{l}{6}f'_0 + f_0 + \frac{K_2}{6EI}\cdot\left(\frac{2l}{6}\right)^3 + \frac{K_3}{6EI}\cdot\left(\frac{4l}{6}\right)^3,$$

and finally we must solve an equation in r_a

$$r_a = \frac{K_3}{\frac{5l}{6}f'_0 + f_0} = \frac{K_2}{f'_0\cdot\frac{3l}{6} + f_0 + \frac{K_3}{6EI}\left(\frac{2l}{6}\right)^3} = \frac{K_1}{\frac{f'_0 l}{6} + f_0 + \frac{K_2}{6EI}\left(\frac{2l}{6}\right)^3 + \frac{K_3}{6EI}\left(\frac{4l}{6}\right)^3},$$

equation which is furnished by the condition

$$Y_1(0) = f_1(0) = 0,$$

or

$$f_0 + \frac{K_1}{6EI} \cdot \left(\frac{l}{6}\right)^3 + \frac{K_2}{6EI} \cdot \left(\frac{3l}{6}\right)^3 + \frac{K_3}{6EI} \cdot \left(\frac{5l}{6}\right)^3 = 0.$$

The value of f'_0 results from calculation of r_a on the basis of the relation furnished by the condition

$$\frac{dy_1}{dx}(0) = f'_1(0) = 0,$$

or

$$f'_0 - \frac{K_1}{2EI} \cdot \left(\frac{l}{6}\right)^2 - \frac{K_2}{2EI} \cdot \left(\frac{3l}{6}\right)^2 - \frac{K_3}{2EI} \cdot \left(\frac{5l}{6}\right)^2 = 0;$$

from this we then will deduce the values of K_1, K_2, K_3.

More generally, a breakdown into $(2n' + 1)$ punctiform masses furnishes a sequence of $(2n' + 1)$ values of K, and consequently $2n'$ relations. The condition

$$y_1(0) = 0$$

furnishes the $(2n' + 1)$th, which is solved by an equation of degree $(2n' + 1)$ in r_a with the value of f'_0 deduced from

$$y'_1(0) = 0.$$

Among the roots of the equation in r_a, at least one of which is real, /47 we select the one which corresponds to the lowest frequency value to obtain the fundamental, and the successive partials are obtained with a precision increasing with n'.

We finally obtain a unique pendular equation whose structure makes it possible to investigate the vibratory blading damping with a controllable precision in calculating elastic stresses; subsequently we will investigate damping, using a very rough approximation of the elastic stresses $(n' = 0)$.

This result shows that it is possible to consider with equal accuracy the centrifugal stresses in accordance with the breakdown given in figure 14. Each elementary mass $\frac{P}{2n' + 1}$ undergoes an acceleration in the direction of increasing x's and equal to

$$\omega_r^2\left(R+\frac{(2q'-1)\,l}{2(2n'+1)}\right);$$

The ratio of the two terms thus demonstrated is

$$\frac{f_c}{F_c}=\frac{(2q'-1)\,l}{2R\cdot(2n'+1)}<\frac{l}{2R}$$

since q' is the order number for the respective mass according to the breakdown adopted, and 2n' + 1 is the total number of the corresponding masses. Having to consider only the relatively short blades (20 cm) set into rotors whose radii easily reach 30 cm, we can neglect the term in $\frac{(2q'-1)\,\omega_r^2\cdot l}{2(2n'+1)}$.

In these expressions, ω_r designates the frequency of machine rotation N_m, or

$$\omega_r = 2\pi N_m.$$

CHAPTER 4. FUNDAMENTAL EQUATION OF VIBRATORY MOTION

4.1 Statement of the Fundamental Equation

In conformance with the diagram of forces in figure 14 corresponding to the case referred to in the preceding chapter, for which n' = 0, we can write (p designating the order number of the respective blade) /48

$$EI\frac{d^2y_p}{dx^2} = \left\{F_y\left(1+\frac{Y_p-Y_{p-1}}{\tau}\right)-P\frac{d^2Y_p}{dl^2}\right\}\left(\frac{l}{2}-x\right)-P\cdot\omega_r^2\cdot R\,(Y_p-y_p) \qquad (20)$$

with

$$y_p = f(x)\,h_p(t), \qquad Y_p = f\left(\frac{l}{2}\right)h_p(t) \quad \text{and} \quad 0 < x \leqslant \frac{l}{2} \quad \text{or} \quad \frac{l}{2} < x \leqslant l.$$

However, this approximation is incorrect for the component of F_y that is a function of time. From formula (15), the increase of circulation $d\gamma$ given in equation (14) is also a function of x through Y_p and the complete statement of equation (20) should include a term in

$$\int_x^l f(x)\,|\,h_p(t)-h_p(t+t_d)\,|\,(X-x)\,dX,$$

which precludes solution with the aid of separate variables. In practice, we will not construct a function Y_p of space and time in successive stages, assuming that the separation of variables presupposes, as indicated in paragraph 3-b of Chapter 3, an experimental adjustment of the damping coefficient. It should be remembered that, during vibration, the exchange of mechanical energy is made between points on the elastic line and that the measurements of the damping coefficient depend strictly on the point of the elastic line selected to carry them out.

In the simplified equation thus obtained, the complement of unity of F_y, $\left(\frac{Y_p - Y_{p-1}}{\tau}\right)$, results from formula (16), with the order of the blades being counted following y. Thus, the balance of the quantities of motion lost in discharge from the rotor, specifically in the case of a circular cascade, will

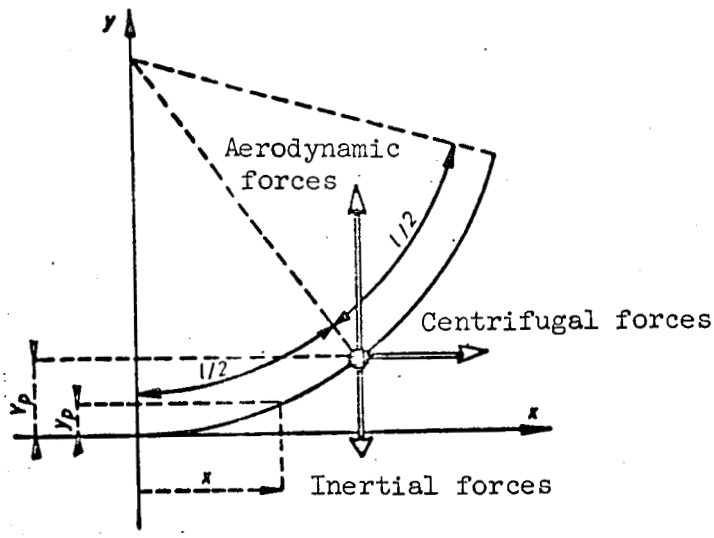

Figure 14

be correct in absolute and in algebraic values. (For example, if $\gamma < 0$, then dF_y is a positive increase of the force applied to the blade of order p, provided the difference $Y_p - Y_{p-1}$ is positive.) /49

Finally, to solve equation (20) we utilize relation (19) resulting from the normalization of the $(2n' + 1)$ equations (19a), (19b), (19c) in the form

$$F_y\left(1 + \frac{Y_p - Y_{p-1}}{\tau}\right) - P\frac{d^2 Y_p}{dl^2} = Kf \cdot P\,\omega_r^2 \cdot R \cdot h_p(l) \tag{19A}$$

with

$$F_y = F_{y_0} + F_{y_1}(l)$$

and equation (20) becomes

$$\frac{EI}{P \cdot \omega_r^2 \cdot R} f''(x) - f(x) = -f\left(\frac{l}{2}\right) - Kf\left(\frac{l}{2} - x\right).$$

This equation is linear and of the second order; hence its general solution

$$\left.\begin{aligned} f(x) &= f\left(\frac{l}{2}\right) - Kf\left(\frac{l}{2} - x\right) + A_0 \operatorname{ch} U_x + B_0 \operatorname{sh} U_x, \quad \text{if} \quad 0 < x \leqslant \frac{l}{2}, \\ f'(x) &= f'\left(\frac{l}{2}\right), \quad \text{if} \quad \frac{l}{2} \leqslant x \leqslant 1, \\ U &= \sqrt{\frac{P \cdot \omega_r^2 \cdot R}{EI}}. \end{aligned}\right\}$$

The determination of A_0 and B_0 results from the limit conditions:

(1) $\frac{dy}{dx}(0) = 0$, or

$$f'(0) = Kf + B_0 U, \qquad B_0 = -\frac{Kf}{U};$$

(2) $y(0) = 0$, or

$$f(0) = f\left(\frac{l}{2}\right) - \frac{Kfl}{2} + A_0 = 0, \qquad A_0 = \frac{Kfl}{2} - f\left(\frac{l}{2}\right);$$

(3) $y(x) = y\left(\frac{l}{2}\right)$ for $x = \frac{l}{2}$, or

$$A_0 \operatorname{ch}\left(\frac{Ul}{2}\right) + B_0 \operatorname{sh}\left(\frac{Ul}{2}\right) = 0,$$

from which

$$\left(Kf\frac{l}{2} - f\left(\frac{l}{2}\right)\right) \operatorname{ch}\frac{Ul}{2} - \frac{Kf}{U}\operatorname{sh}\left(\frac{Ul}{2}\right) = 0;$$

$$Kf = k^2 \frac{f\left(\frac{l}{2}\right)}{\frac{l}{2}}; \qquad k^2 = \frac{1}{1 - \frac{\operatorname{th}\frac{Ul}{2}}{\frac{Ul}{2}}}.$$

Equation (19A) in h_p is therefore written as

$$F_y\left\{1 + \frac{f\left(\frac{l}{2}\right)\cdot(h_p - h_{p-1})}{\tau}\right\} - P \cdot f\left(\frac{l}{2}\right)\cdot h''_p = k^2 \frac{f\left(\frac{l}{2}\right)}{\frac{l}{2}} \cdot P\,\omega_r^2\,R \cdot h_p,$$

or

$$lh''_p + \left\{2k^2 \cdot \omega_r^2\,R - \frac{l}{\tau}\cdot\frac{F_y}{P}\right\}\cdot h_p = \frac{l}{f\left(\frac{l}{2}\right)}\cdot\frac{F_y}{P}\cdot\left\{1 - \frac{f\left(\frac{l}{2}\right)}{\tau}h_{p-1}\right\} \qquad (19B)$$

which is the fundamental equation desired if we disregard the damping action of metallic friction.

4.2 Natural Frequency of an Isolated Blade

From equation (19B) it is possible to reproduce the natural frequency of the isolated blade within a fluid at rest, i.e., the one measured in practice on the machine rotor at rest; to achieve this, the term representing the centrifugal forces in $\omega_r^2 R$ and the terms representing the aerodynamic forces in F_y must be made to tend toward zero.

Let us state /51

$$U_0 = \frac{Ul}{2}$$

and let us consider the limited development

$$\frac{\text{th } U_0}{U_0} = \frac{U_0 + \frac{U_0^3}{3!} + \frac{U_0^5}{5!} + \cdots}{U_0\left(1 + \frac{U_0^2}{2!} + \frac{U_0^4}{4!} + \cdots\right)} = 1 - \left(\frac{1}{2!} - \frac{1}{3!}\right) U_0^2 + \cdots.$$

This development allows us to write

$$1 - \frac{\text{th } U_0}{U_0} \neq \frac{U_0^2}{3} = \frac{P \cdot \omega_r^2 \cdot R}{EI} \cdot \frac{l^2}{4} \cdot \frac{1}{3},$$

from which

$$2 \cdot k^2 \cdot \omega_r^2 \cdot R = \frac{24\,EI}{Pl^2}$$

and equation (19B) becomes

$$lh'' + \frac{24\,EI}{Pl^2} h = 0,$$

from which we deduce the natural frequency (as a very rough approximation here)

$$N_p = \frac{1}{2\pi}\sqrt{\frac{24\,EI}{Pl^3}}.$$

This is the fundamental equation. The partial equations are obtained with a more complex formulation as indicated in Chapter 3 and, with them, a value of N_p as much more accurate as they are numerous.

4.3 Approximate Linearity of the Fundamental Equation

The linear character of the fundamental equation results from the division in two parts of γ given in regard to equation (15B), which makes it possible to write

$$F_y = F_{y_0} + F_{y_1}(t),$$

and consequently, in equation (19B)

$$l\,h''_p(t) + 2 \cdot k^2 \cdot \omega_r^2 \cdot R \cdot h_p(t) - \frac{l}{\tau}\frac{F_{y_0}}{P} h_p(t) - \frac{l}{\tau} \cdot \frac{F_{y_1}(t)}{P} \cdot h_p(t)$$

$$= \frac{lF_{y_0}}{P \cdot f\left(\frac{l}{2}\right)} + \frac{lF_{y_1}(t)}{P \cdot f\left(\frac{l}{2}\right)} - \frac{l}{\tau} \cdot \frac{F_{y_0}}{P} \cdot h_{p-1}(t) - \frac{l}{\tau}\frac{F_{y_1}(t)}{P} h_{p-1}(t).$$

From formula (15B), γ_1 is an infinitesimal of the first order and, consequently, the term in $F_{y_1}(t)$ in the first member is negligible in relation to the term in F_y. Similarly, the term in $F_{y_1}(t)\, h_{p-1}(t)$ in the second member is negligible in relation to the term in $F_{y_0}\, h_{p-1}(t)$. In addition we shall /52 see in detail in Chapter 5 how decomposition of the product $\gamma_1 \sin(\omega t + j)$ included in $\frac{F_{y_1}(t)}{f\left(\frac{l}{2}\right)}$ introduces into the first member a term in $\frac{dh_p(t)}{dt}$ and a term in $h_p(t)$. It will suffice here to stress that, by stating F_y explicitly as a function of γ_1, we give equation (19B) the form

$$ah''_p + bh'_p + \left\{c - \frac{qW_1}{\sqrt{1 - M^2} \cdot p} \cdot \frac{\sin\psi}{\cos(\psi - m)} \cdot \frac{l}{\tau}\right\} h_p$$

$$= -\frac{qW_1}{\sqrt{1 - M^2} \cdot p} \cdot \frac{\sin\psi}{\cos(\psi - m)} \cdot \frac{l}{\tau}$$

$$+ \frac{qW_1 \cdot l}{\sqrt{1 - M^2} \cdot P \cdot f\left(\frac{l}{2}\right)} \cdot \frac{|\psi| \cdot d_p(\mathrm{Re})}{\cos^2(\psi - m)} \cdot 2 \sin\frac{\omega l_d}{2} \cdot \cos\left(\omega l + \frac{l_d}{2}\right)$$

$$- \frac{qW_1}{\sqrt{1 - M^2} \cdot p} \cdot \frac{\sin\psi}{\cos(\psi - m)} \cdot \frac{l}{\tau} \cdot h_{p-1}(t),$$

or

$$ah''_p + bh'_p + (c + I_e)\,h_p = d + I_e \cdot h_{p-1} + f \sin\left(\omega t + j - \frac{2p\pi}{N_0}\right), \qquad (19C)$$

by taking into account the relation (15A) and by introducing a phase-shift function of order p defined in the following section, which is zero for the blade of the order N_0. We thus have

$$I_e = -\frac{m_s W_1^2 \cdot l^2}{\sqrt{1 - M^2 \cdot P}} \cdot \frac{\sin\psi \cos m}{\cos(\psi - m)},$$

$$f = \frac{m_s \cdot W_1^2 \cdot l^2}{\sqrt{1 - M^2 \cdot P}} \cdot \frac{\tau}{e} \cdot \frac{\cos^2\theta_1 \cdot \cos^2 m}{\cos^2(\psi - m)} \cdot \frac{c_d \cdot |\psi| \cdot d_p(\mathrm{Re})}{f\left(\frac{l}{2}\right) \cdot \cos\theta_1} \cdot 2\sin\frac{\omega t_d}{2}.$$

We can already note that the coefficients a and c of equation (19C) are written, in the absence of aerodynamic stresses, as

$$a = l; \qquad c = 2k^2 \cdot \omega_r^2 \cdot R; \qquad \frac{c}{a} = \omega_0^2.$$

It is also important to note that equation (19C) contains only a term of self-excitation due to the wake of the profiles, and does not take into account any other excitation forces. These forces result most often from breakdown of the flux of a development in a Fourier series (ref. 25) in relation to the multiples of the excitation frequency, and the presence of these forces may be expressed by frequency and amplitude modulation of the vibratory phenomena due to self-excitation when the orders of magnitude are comparable.

Finally, we should further stress that the frequency ω appearing in the second member, i.e., the vibratory frequency of the respective blade, is a priori different from the natural blade frequency ω_0 which can be observed by revolving the rotor in vacuum taking into account the centrifugal forces.

4.4 Investigation of the System of Equations (19) Representing the Vibrations of All the Blades in the Cascade

Equation (19C) is included in a system which consists of as many equations as the cascade has blades /53

$$
\left.
\begin{aligned}
& ah''_1 + bh'_1 + (c + I_e)\, h_1 = d + I_e\, h_{N_0} + f \sin\left(\omega t + j - \frac{2\pi}{N_0}\right); && 19.1 \\
& ah''_2 + bh'_2 + (c + I_e)\, h_2 = d + I_e\, h_1 + f \sin\left(\omega t + j - \frac{4\pi}{N_0}\right); && 19.2 \\
& \cdots\cdots\cdots\cdots\cdots\cdots\cdots\cdots\cdots\cdots\cdots\cdots\cdots\cdots\cdots\cdots\cdots\cdots\cdots\cdots\cdots\cdots \\
& ah''_p + bh'_p + (c + I_e)\, h_p = d + I_e\, h_{p-1} + f \sin\left(\omega t + j - \frac{2p\pi}{N_0}\right); && 19.p \\
& \cdots\cdots\cdots\cdots\cdots\cdots\cdots\cdots\cdots\cdots\cdots\cdots\cdots\cdots\cdots\cdots\cdots\cdots\cdots\cdots\cdots\cdots \\
& ah''_{N_0-1} + bh'_{N_0-1} + (c + I_e)\, h_{N_0-1} = d + I_e\, h_{N_0-2} && 19.N_0-1 \\
& \qquad + f \sin\left(\omega t + j - \frac{2[N_0-1]\pi}{N_0}\right); \\
& ah''_{N_0} + bh'_{N_0} + (c + I_e)\, h_{N_0} = d + I_e\, h_{N_0-1} && 19.N_0 \\
& \qquad + f \sin\left(\omega t + j - \frac{2[N_0]\pi}{N_0}\right).
\end{aligned}
\right\} \qquad (19)
$$

In the case of a circular cascade, the phase shift $\frac{2\pi}{N_0}$ between the vibrations of two consecutive blades, which is assumed in the formulation of such system, is the consequence of a simplifying hypothesis according to which the cascade and the flow passing through it are perfectly symmetrical in a symmetry in $\frac{2\pi}{N_0}$. The phase shift of one blade in relation to itself is equal to 2π and, if we admit that the phase shift at the p-th blade in relation to the (p - 1)th blade is equal to the phase shift of the (p + 1)th blade in relation to the p-th blade, it is clear that the phase shift then must be equal to $\frac{2\pi}{N_0}$. In practice, we occasionally observe phase shift values between consecutive blades equal to $\frac{2m_0\,\pi}{N_0}$, which leads to the assumption that phase shift of one blade in relation to itself is $2m_0\,\pi$, where m_0 is a whole number.

In the case of a rectilinear cascade of the type investigated in Chapter 2, we can identically conclude this by assuming that the first and the last blade were placed at a distance from the wind tunnel walls equal to the cascade pitch.

A. General Solution of the Equation for Vibration Without the Second Member

Solution by successive substitution leads to a linear differential equation with constant coefficients on the order of $2N_0$ in h_{N_0}, whose second member is a periodic function of ωt. The corresponding characteristic equation is

$$ar^2 + br + c + I_e)^{2N_0} - I_e^{2N_0} = 0. \tag{21}$$

Each h_p function constituting the desired solution is therefore obtained from a single equation with the characteristic values /54

$$ar^2 + br + c = 0, \tag{22}$$

Thus, all the preceding applies to each blade of the same cascade, and specifically the calculation of the damping coefficient, in the form

$$\frac{\pi b}{\sqrt{a \cdot c}}.$$

B. Special Solution of System (19) when the Equations are Written with their Second Member

Within a certain approximation which will be as much better as the number N_0 of the blades of the cascade is greater, system (19) permits the following special solution

$$\left.\begin{aligned} h_p &= h_\infty \cdot \sin\left(\omega t - \frac{2p\pi}{N_0}\right) + \frac{d}{c}; && 23.1 \\ h_\infty &= \frac{f \cdot \cos j}{c - a\omega^2}; && 23.2 \\ \operatorname{tg} j &= \frac{b\omega}{c - a\omega^2}. && 23.3 \end{aligned}\right\} \tag{23}$$

We thus have

$$h_{p-1} = h_\infty \cdot \sin\left(\omega t - \frac{2(p-1)\pi}{N_0}\right) + \frac{d}{c},$$

$$h'_p = h_\infty \cdot \omega \cdot \cos\left(\omega t - \frac{2p\pi}{N_0}\right),$$

$$h''_p = -h_\infty \cdot \omega^2 \sin\left(\omega t - \frac{2p\pi}{N_0}\right),$$

and consequently, by substitution in equation (19C)

$$h_\infty \cdot (c - a\,\omega^2) \sin\left(\omega t - \frac{2\,p\,\pi}{N_0}\right) + b \cdot h_\infty \cdot \omega \cdot \cos\left(\omega t - \frac{2\,p\,\pi}{N_0}\right) + \frac{(c + I_e)\,d}{c}$$
$$= d + \frac{I_e\,d}{c} + I_e \cdot h_\infty \cdot \sin\left(\omega t - \frac{2\,(p-1)\,\pi}{N_0}\right) - I_e\,h_\infty \cdot \sin\left(\omega t - \frac{2\,p\,\pi}{N_0}\right)$$
$$+ f \cdot \sin\left(\omega t - \frac{2\,p\,\pi}{N_0}\right)\cos j + f \cdot \cos\left(\omega t - \frac{2\,p\,\pi}{N_0}\right)\sin j.$$

In this last equation, the introduction of relation (23.2) yields

$$I_e \cdot h_\infty \cdot \left\{ \sin\left(\omega t - \frac{2\,p\,\pi}{N_0}\right) - \sin\left(\omega t - \frac{2\,(p-1)\,\pi}{N_0}\right) \right\}$$
$$= f \sin j - b \cdot h_\infty \cdot \omega \left\{ \cos\left(\omega t - \frac{2\,p\,\pi}{N_0}\right), \right.$$

or also, considering relation (23.3)

$$2 \cdot I_e \cdot h_\infty \cdot \sin\frac{\pi}{N_0} \cdot \cos\left(\omega t - \frac{2\,p-1}{2} - \frac{\pi}{N_0}\right) = 0.$$

This last identity is ascertained within the second order, since I_e is an infinitesimal of the first order, as is the deviation angle ψ, when N_0 is sufficiently large so that $\frac{\pi}{N_0}$ itself is an infinitesimal of the first order ($\sin\frac{\pi}{N_0} = 0.26$ for $N_0 = 12$). /55

C. Complete Solution of the Fundamental Equation

From the foregoing, solution is obtained by superimposing the special solution (23) on the general solution of equation

$$ah'' + bh' + ch = 0,$$

which results in the study of damping and of stability which are the subject of Chapter 5.

This method of solution obviously supposes that the initial conditions at the time of release of the cascade blades are particular. In the more general case, the characteristic equation must be treated as an equation with multiple roots. Also, $2N_0$ solutions for the equation without second member can each be found separately by constituting exponential products using polynomials. The

particular case under consideration is the one in which the constant factors affecting these products are zero.

We are satisfied with this particular case because the instabilities which would not come under any predetermined initial conditions system would have no physical significance and would not exist in practice.

CHAPTER 5. INVESTIGATION OF DAMPING

The preceding chapters make it possible to limit the investigation to /56
that of the typical equation

$$ah'' + bh' + ch = f \sin(\omega t + j).$$

The coefficient b of $\frac{dh}{dt}$ is the sum of two elements b_1 and b_2. The more important, b_1, results from formulas (15) and (15B).

We return to equation (19B)

$$lh'' + \left(2k^2 \cdot \omega_r^2 \cdot R - \frac{l}{\tau}\frac{F_y}{P}\right)h = \frac{l}{f\frac{l}{2}} \cdot \frac{F_y}{P}\left\{1 - \frac{f\left(\frac{l}{2}\right)}{\tau} h_{p-1}\right\}$$

and the definition of F_y given in Chapter 4

$$F_y = -\frac{q \cdot \gamma_0}{\tau} - \frac{q \cdot \gamma_1}{\tau} \cdot \sin(\omega t + j).$$

We thus have

$$F_y = F_{y_0} + \begin{cases} \dfrac{-q \cdot W_1 \cdot \cos m}{\sqrt{1 - M^2} \cdot e} \cdot \dfrac{\cos^2 \theta_1}{\cos^2(\psi - m)} \cdot \left\{\dfrac{1}{\omega} \cdot \sin \omega t_d \cdot \dfrac{dy_p}{dt} - 2 \sin^2 \dfrac{\omega t_d}{2} \cdot y_p\right\} \\ + \dfrac{q \cdot W_1 \cdot \cos m}{\sqrt{1 - M^2} \cdot e} \cdot \dfrac{\cos^2 \theta_1}{\cos^2(\psi - m)} \cdot \dfrac{c_d |\psi| \cdot d_p(\mathrm{Re})}{\cos \theta_1} \cdot 2 \sin \dfrac{\omega t_d}{\tau} \cdot \cos \omega\left(t + \dfrac{t_d}{\tau}\right) \end{cases}$$

and without damping we would have in these expressions

$$y_p = f\left(\frac{l}{2}\right) h_p = f\left(\frac{l}{2}\right) \cdot \sin \omega t, \qquad q = m_s \cdot \tau \cdot l \cdot W_1 \cdot \cos m,$$

or since h_p is a function slowly variable in time,

$$\frac{lF_y}{P \cdot l\left(\frac{l}{2}\right)} = \frac{lF_0}{Rl\left(\frac{l}{2}\right)}$$

$$+\left\{\begin{array}{l} -\dfrac{m_s \cdot l^2 \cdot W_1^2}{P\sqrt{1-M^2}} \cdot \dfrac{\tau}{e} \cdot \dfrac{\cos^2\theta_1 \cdot \cos^2 m}{\cos^2(\psi - m)}\left(\dfrac{1}{\omega} \cdot \sin \omega t_d \cdot \dfrac{dh_p}{dt} - 2 \cdot \sin^2 \dfrac{\omega t_d}{2} \cdot h_p\right) \\ +\dfrac{m_s \cdot l^2 \cdot W_1^2}{P\sqrt{1-M^2}} \cdot \dfrac{\tau}{e} \cdot \dfrac{\cos^2\theta_1 \cos^2 m}{\cos^2(\psi - m)} \cdot \dfrac{c_d |\psi| \cdot d_p (\mathrm{Re})}{\cos\theta_1} \cdot 2 \sin \dfrac{\omega t_d}{\tau} \cdot \cos \omega\left(t + \dfrac{t_d}{2}\right) \end{array}\right.$$

from which we deduce

$$b_1 = \frac{m_s \cdot l^2 \cdot W_1^2}{P\sqrt{1-M^2}} \cdot \frac{\tau}{e} \cdot \frac{\cos^2\theta_1 \cdot \cos^2 m}{\cos^2(\psi - m)} \cdot \frac{1}{\omega} \sin \omega t_d,$$

$$c = 2 \cdot k^2 \cdot \omega_r^2 R - \frac{m_s \cdot l^2 \cdot W_1^2}{P\sqrt{1-M^2}} \cdot \frac{\tau}{e} \cdot \frac{\cos^2\theta_1 \cdot \cos^2 m}{\cos^2(\psi - m)} \cdot 2 \sin^2 \frac{\omega t_d}{2},$$

$$l \sin(\omega t + j) = \frac{m_s \cdot l^2 \cdot W_1^2}{P\sqrt{1-M^2}} \cdot \frac{\tau}{e} \cdot \frac{\cos^2\theta_1 \cdot \cos^2 m}{\cos^2(\psi - m)} \cdot \frac{c_d \cdot |\psi| \cdot d_p (\mathrm{Re})}{l\left(\frac{l}{2}\right) \cdot \cos\theta_1} 2 \sin \frac{\omega t_d}{2} \cdot \cos \omega\left(t + \frac{t_d}{2}\right).$$

The second element, b_2, representing the material's internal damping, /57 can be conveniently expressed by the logarithmic decrement of vibrations observed in still air with the rotor stopped

$$b_2 = \frac{d_0}{\pi} \sqrt{a \cdot c}.$$

To sum up, the investigation must proceed from equation

$$ah'' + bh' + ch = l \sin(\omega t + j) \qquad (19D)$$

with the following coefficients

$$
\left.
\begin{aligned}
a &= l, \\
b &= \frac{d_0}{\pi}\sqrt{a \cdot c} - \frac{m_s \cdot l^2 \cdot W_1^2}{P\sqrt{1-M^2}} \cdot \frac{\tau}{e} \cdot \frac{\cos^2\theta_1 \cdot \cos^2 m}{\cos^2(\psi - m)} \cdot \frac{1}{\omega} \sin \omega t_d, \\
c &= 2 \cdot k^2 \cdot \omega_r^2 \cdot R - \frac{m_s \cdot l^2 \cdot W_1^2}{P\sqrt{1-M^2}} \cdot \frac{\tau}{e} \cdot \frac{\cos^2\theta_1 \cdot \cos^2 m}{\cos^2(\psi - m)} \cdot 2 \sin^2 \frac{\omega t_d}{2}, \\
j &= -\frac{\pi}{2} + \frac{\omega t_d}{2}, \\
f &= \frac{m_s \cdot l^2 \cdot W_1^2}{P\sqrt{1-M^2}} \cdot \frac{\tau}{e} \cdot \frac{\cos^2\theta_1 \cdot \cos^2 m}{\cos^2(\psi - m)} \cdot \frac{c_d \,|\, \psi \,|\, \cdot d_p(\mathrm{Re})}{f\left(\frac{l}{2}\right) \cdot \cos\theta_1} \cdot 2 \sin \frac{\omega t_d}{2}.
\end{aligned}
\right\} \qquad (24)
$$

5.1 Vibratory Frequency is Equal to Natural Frequency

From formulas (23.3) and (15A) we have

$$
c - a\omega^2 = b\omega \operatorname{cotg} j = -b\omega \operatorname{tg} \frac{\omega t_d}{2},
$$

or, by deriving a, b and c from relations (24)

$$
\omega_0^2 l \cdot \frac{m_s \cdot l^2 \cdot W_1^2}{P\sqrt{1-M^2}} \cdot \frac{\tau}{e} \cdot \frac{\cos^2\theta_1 \cdot \cos^2 m}{\cos^2(\psi - m)} \cdot 2 \sin^2 \frac{\omega t_d}{2} - l\omega^2
$$

$$
= -\frac{\sin \frac{\omega t_d}{2}}{\cos \frac{\omega t_d}{2}} \left\{ \frac{d_0 l \omega}{\pi} \omega_0 + \frac{m_s \cdot l^2 \cdot W_1^2}{P\sqrt{1-M^2}} \cdot \frac{\tau}{e} \cdot \frac{\cos^2\theta_1 \cdot \cos^2 m}{\cos^2(\psi - m)} \cdot \sin \omega t_d \right\}.
$$

or

$$
\omega_0^2 - \omega^2 = -\omega^2 \frac{d_0}{2\pi} \cdot \omega_0 t_d \sim 0,
$$

since the true frequency ω is in principle only slightly higher than the natural frequency. /58

The natural frequency ω_0 is by definition

$$
\omega_0 = \sqrt{2k^2 \frac{\omega_r^2 R}{l}}.
$$

5.2 With No Self-Exciting Force Due to Detachment at the Profile Tip, the Fluid Damps the Blading Vibrations

The second of relations (24) allows us to define the damping coefficient in the form

$$A_m = \frac{\pi b}{\sqrt{a \cdot c}} = \frac{\pi b}{a \cdot \omega} = \frac{\pi b}{l \cdot \omega},$$

$$A_m = d_0 + \frac{m_s \cdot l \cdot \tau \cdot W_1^2}{P\sqrt{1 - M^2}} \cdot \frac{\cos^2 m \cos^2 \theta_1}{\cos^2 (\psi - m)} \cdot \frac{\pi}{e\,\omega^2} \cdot \sin \omega t_d$$

with definition of the time of passage t_d given for formulas (15)

$$t_d = \frac{c_d}{W_m} = \frac{e}{W_m \cdot \cos \theta_1}$$

and with no account of an experimental proportional adjustment.

Figure 7 furnishes the geometric elements for calculation of W_m as a function of W_1, m and ψ through application of the bisector theorem

$$2 W_m^2 = W_1^2 + W_1^2 \frac{\cos^2 m}{\cos^2 (\psi - m)} - W_1^2 \frac{\sin^2 \psi}{2 \cos^2 (\psi - m)},$$

$$W_m = \frac{W_1}{\sqrt{2}} \frac{\sqrt{\cos^2 (\psi - m) + \cos^2 m - 0{,}5 \sin^2 \psi}}{\cos (\psi - m)}$$

from which

$$\omega \cdot l \cdot d = \frac{e\,\omega}{W_1 \cos \theta_1} \frac{\sqrt{2} \cdot \cos (\psi - m)}{\sqrt{\cos^2 (\psi - m) + \cos^2 m - 0{,}5 \sin^2 \psi}}$$

and formula (25)

$$A_m - d_0 = \frac{m_s \cdot l \cdot W_1^2}{P\sqrt{1 - M^2}} \cdot \frac{\cos^2 m \cdot \cos^2 \theta_1}{\cos^2 (\psi - m)} \cdot \frac{\pi \tau}{e\,\omega^2}$$

$$\times \sin \left\{ \frac{\omega}{W_1 \cos \theta_1} \cdot \frac{\sqrt{2} \cos (\psi - m)}{\sqrt{\cos^2 (\psi - m) - \cos^2 m - 0.5 \sin^2 \psi}} \right\}.$$

The formula shows that, without any self-exciting forces, the fluid itself damps the vibrations of the blading approximately proportionally to the incident velocity. /59

5.3 A Self-Exciting Force Can Lead to Negative Values of the Damping Coefficient

To construct the general solution for equation (19C), it is necessary, as shown in Chapter 4, to solve the equation with no second member

$$ah'' + \frac{A_m}{\pi}\sqrt{a \cdot c}\, h' + ch = 0$$

which furnishes

$$h = e^{-\frac{Am}{2\pi}\omega_0 t}(T_1 \cos \omega_1 t + T_2 \sin \omega_1 t)$$

with

$$\omega_1 = \omega_0 \sqrt{1 - \frac{A_m^2}{4\pi^2}}$$

and this general solution appears in the form

$$h = e^{-\frac{Am}{2\pi}\omega_0 t}(T_1 \cos \omega_1 t + T_2 \sin \omega_1 t) + h_\infty \sin \omega t, \tag{26}$$

where T_2 and T_1 are determined by the initial conditions

$$h = 1 \quad \text{for} \quad t = 0, \quad \text{or} \quad T_1 = 1 \quad \text{and} \quad \frac{dh}{dt} = 0 \quad \text{for} \quad t = 0.$$

However

$$\frac{dh}{dt} = e^{-\frac{Am}{2\pi}\omega t}\{-T_1 \cdot \omega_1 \sin \omega_1 t + T_2 \omega_1 \cdot \cos \omega_1 t\}$$

$$-\frac{A_m}{2\pi} \cdot \omega_0 \cdot e^{-\frac{Am}{2\pi}\omega t}\{T_1 \cos \omega_1 t + T_2 \cdot \sin \omega_1 t\} + h_\infty \cdot \omega \cdot \cos \omega t,$$

from which

$$T_2 \omega_1 - \frac{A_m}{2\pi} \cdot \omega_0 T_1 + h_\infty \cdot \omega = 0,$$

or

$$T_2 = \frac{A_m}{2\pi} \cdot \frac{\omega_0}{\omega_1} - h_\infty \frac{\omega}{\omega_1}.$$

We simplify by taking

$$\omega_1 \# \omega_0 \# \omega.$$

We then find /60

$$h = e^{-\frac{A_m}{2\pi}\omega t}\left\{\cos\omega t + \left(\frac{A_m}{2\pi} - \frac{h_\infty}{h_0}\right)\sin\omega t\right\} + h_\infty \cdot \sin\omega t, \tag{27}$$

or, multiplying the two members of the equation by $f\left(\frac{1}{2}\right)$

$$y = y_0 e^{-\frac{A_m}{2\pi}\omega t}\left\{\cos\omega t + \left(\frac{A_m}{2\pi} - \frac{y_\infty}{y_0}\right)\cdot \sin\omega t\right\} + y_\infty \sin\omega t. \tag{28}$$

It is then convenient to express the ratio $\frac{y}{y_0}$ in the form of the product of a sine by an aperiodic time function representing evolution of the pseudo-amplitude y_M, and consequently defining the corresponding damping

$$\frac{y}{y_0} = \left\{e^{-\frac{A_m}{2\pi}\omega t}\left(\frac{A_m}{2\pi} - \frac{y_\infty}{y_0}\right) + \frac{y_\infty}{y_0}\right\}\sin\omega t + e^{-\frac{A_m}{2\pi}\omega t}\cdot\cos\omega t$$

or

$$\frac{\frac{y}{y_0}}{\sqrt{\left\{e^{-\frac{A_m}{2\pi}\omega t}\left(\frac{A_m}{2\pi} - \frac{y_\infty}{y_0}\right) - \frac{y_\infty}{y_0}\right\}^2 + e^{-\frac{A_m}{\pi}\omega t}}} = \sin\left\{\omega t + \operatorname{arctg}\frac{1}{\left(\frac{A_m}{2\pi} - \frac{y_\infty}{y_0}\right) + \frac{y_\infty}{y_0}e^{-\frac{A_m}{2\pi}\omega t}}\right\}, \tag{29}$$

which gives

$$\frac{y_M}{y_0} = \sqrt{\left\{e^{-\frac{A_m}{2\pi}\omega t}\left(\frac{A_m}{2\pi} - \frac{y_\infty}{y_0}\right) + \frac{y_\infty}{y_0}\right\}^2 + e^{-\frac{A_m}{\pi}\omega t}}. \tag{30}$$

Consequently, a condition necessary for negative damping to succeed positive damping during blading operation is

$$1 > \frac{y_\infty}{y_0} > \frac{A_m}{2\pi}.$$

and we shall see that it is sufficient.

Let us first note that where

$$y_0 < y_\infty,$$

damping is negative upon release into the wind at amplitude y_0; in the opposite case this condition must suffice so that the equation

$$\frac{y_м}{y_0} - \frac{y_\infty}{y_0} = 0, \tag{31}$$

satisfied in all cases where $t \to \infty$, admits another positive root in t, or else so that /61

$$\left\{ e^{-\frac{Am}{2\pi}\omega t} \cdot \left(\frac{A_m}{2\pi} - \frac{y_\infty}{y_0}\right) + \frac{y_\infty}{y_0} \right\}^2 + e^{-\frac{Am}{\pi}\omega t} = \left(\frac{y_\infty}{y_0}\right)^2$$

or

$$\left(\frac{A_m}{2\pi} - \frac{y_\infty}{y_0}\right)^2 + 2e^{-\frac{Am}{2\pi}\omega t} \cdot \left(\frac{A_m}{2\pi} - \frac{y_\infty}{y_0}\right) \cdot \frac{y_\infty}{y_0} + 1 = 0 \tag{32}$$

$$e^{-\frac{Am}{2\pi}\omega t} = \frac{1 + \left(\frac{y_\infty}{y_0} - \frac{A_m}{2\pi}\right)^2}{2\left(\frac{y_\infty}{y_0} - \frac{A_m}{2\pi}\right) \cdot \frac{y_\infty}{y_0}}$$

It does suffice because it makes the second member of equation (32) positive and permits expression of the logarithm of its two members.

To use equation (32), it is convenient to specify y_∞ by comparing the last relation in (24) and relation (25), where we find that

$$f = (A_m - d_0) \cdot \frac{\omega^2}{\pi} \cdot \frac{c_d \cdot |\psi| \cdot d_p(\mathrm{Re})}{l\left(\frac{l}{2}\right) \cdot \cos\theta_1},$$

from which

$$h_\infty = \frac{f \cdot \cos j}{c - a\omega^2} = \frac{f \cdot \sin j}{b\omega} \sim \frac{f}{b\omega},$$

$$y_\infty = \left(1 - \frac{d_0}{A_m}\right) \cdot \frac{c_d \cdot |\psi| \cdot d_p(\mathrm{Re})}{\cos\theta_1}. \tag{33}$$

CHAPTER 6. COMPARISON WITH EXPERIMENT
CORRESPONDENCE BETWEEN NOTATIONS

With the results obtained during the investigation presented here, it /62 seems possible to interpret the experiments made in the cascade wind tunnel at Chalais-Meudon by M. Leclerc, Research Engineer at ONERA, and reported in Recherche Aéronautique, No. 71 (July-August 1959).

Figure 15 shows the cascade's overall configuration.

Figure 16 gives the geometric elements of these experiments and figure 17 gives the same representation with the notations from the study. The table at the end of this section specifies this correspondence.

Figures 18 and 19 subsequently specify the e_f sign whose absolute value is no other, in the total absence of detachment, than one-half the angle at the apex of the profile tip:

$$\text{absolute value of } e_f \# \frac{1}{10} \# 6^\circ.$$

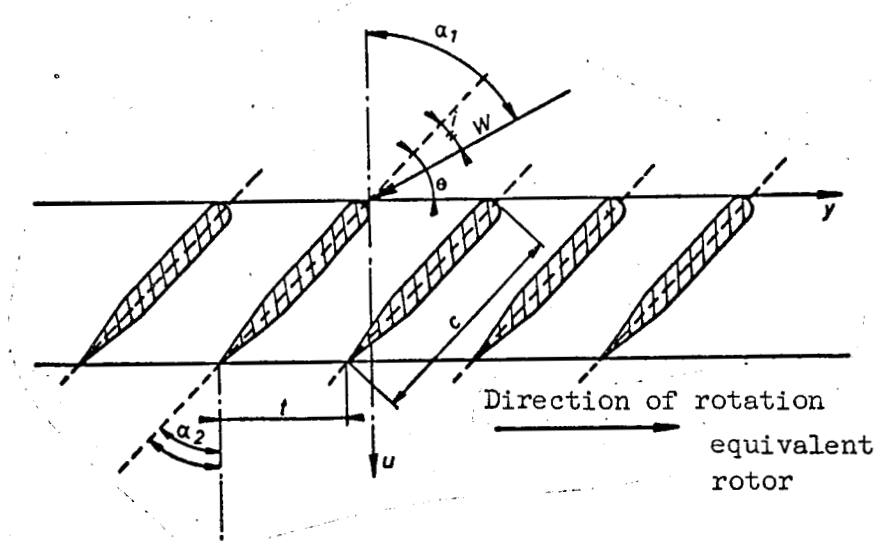

Figure 15

t, Pitch; c, chord; $h = \frac{t}{c}$, reduced pitch; θ, setting = 45°;

i, incidence (positive on deceleration cascade as in figure).

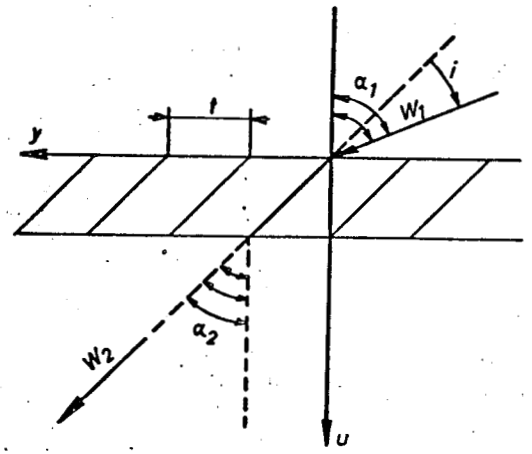

Figure 16

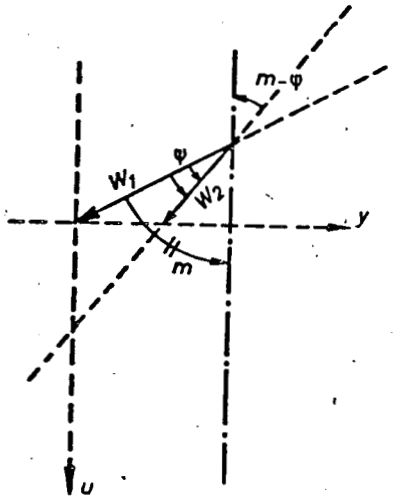

Figure 17

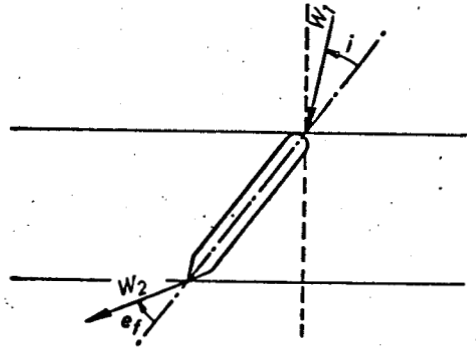

Figure 18

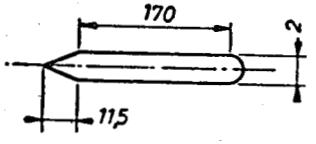

Figure 18A

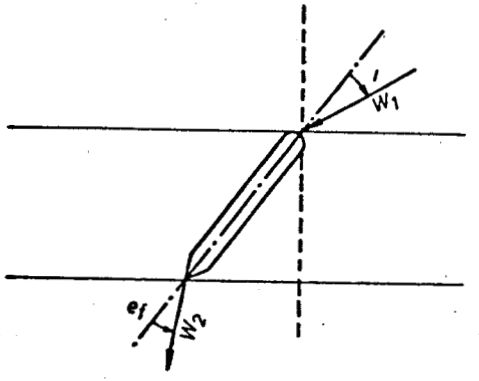

Figure 19

Designation	Theoretical notations	Experimental notations
Relative incident velocity ..	W_1	V
Inclination of W_1 on O_u	$-m$	$i+\frac{\pi}{4}=\alpha_1$
Inclination of W_2 on O_u	$m-(\psi)$	$-\frac{\pi}{4}\pm e_f=-\alpha_2$
Mean fluid deviation	ψ	$-1\pm e_f$
Profile setting	θ_1	$\theta=\frac{\pi}{4}$
Absolute pitch	(τ)	t
Profile chord	c_d	c
Reduced pitch	$\frac{\tau}{c_d}$	h

Even though approximate, the actual value of e_f can be deduced from the curves giving the variations of the number of pressure at constant velocity and variable incidence such as figure 6 on page 61 of Recherche Aéronautique No. 71. /64

6.1 Demonstration of Detachment

From the expression of the number of pressure

$$N_b = 1 - \left\{ \frac{\cos\left(i+\frac{\pi}{4}\right)}{\cos\left(\frac{\pi}{4}\pm e_f\right)} \right\}^2$$

we derive the value of

$$\cos\left(\frac{\pi}{4}\pm e_f\right) = \frac{\cos\left(i+\frac{\pi}{4}\right)}{\sqrt{1-N_b}}.$$

Table 5 and figure 20 give graphic representation of this and show that the tested blading actually operates in expansion ($\alpha_2 > \alpha_1$) for values of the incidence i between zero and -15°. When incidence is positive, the intake and discharge angles are practically equal, i.e., transition from the configuration in figure 18 to that in figure 19 does not occur, thus indicating that only negative incidence can validly be considered.

By a scale change, figure 20A shows that when incidence assumes increasingly high values, the difference ψ ceases to increase with incidence, i.e., the

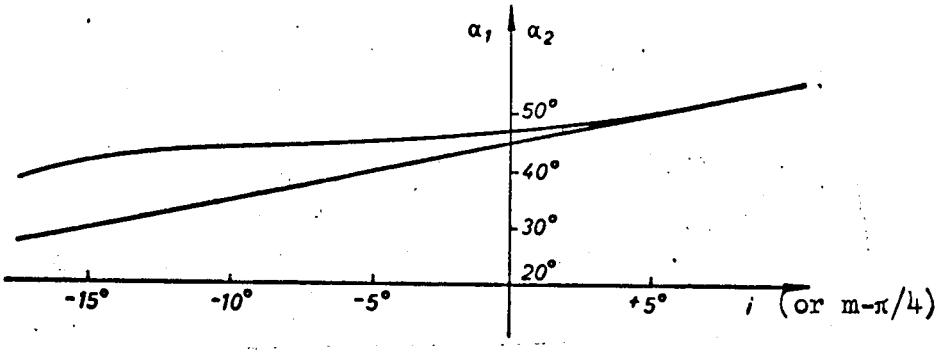

Figure 20

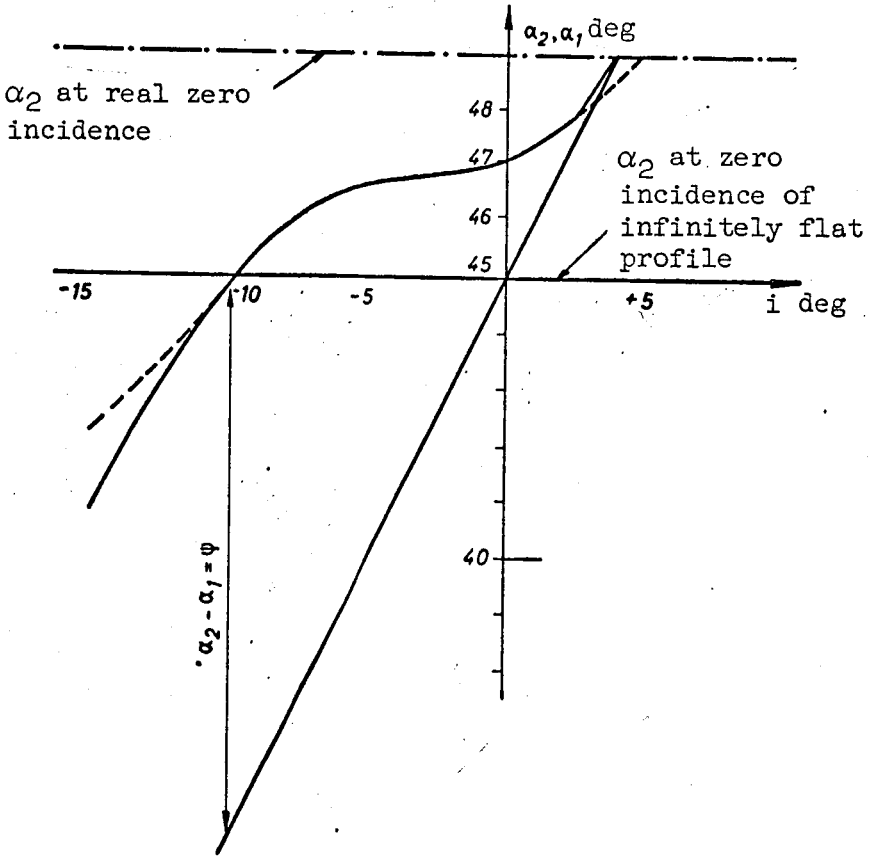

Figure 20A

localized detachments responsible for introduction of the term in $d_p(Re)$ tend to be generalized and that, simultaneously, any supplementary energy transfer of fluid to blading occurs in a disordered manner, specifically in a vibratory form intermediate between the thermal and mechanical forms usable in the machine shaft.

TABLE 5

i	— 15	— 10	— 7°30	— 5	— 2°30	0	5°
$\alpha_1 = i + \frac{\pi}{4}$	30°	35°	37°30	40°	42°30	45°	50°
N_b	— 0,375	— 0,340	— 0,310	— 0,245	— 0,165	— 0,080	0,030
$1 - N_b$	1,375	1,340	1,310	1,245	1,165	1,080	0,97
$\cos\left(i + \frac{\pi}{4}\right)$	0,8660	0,8191	0,7934	0,7660	0,7373	0,7071	0,6428
$\sqrt{1 - N_b}$	1,173	1,158	1,144	1,116	1,075	1,039	0,9987
$\cos \alpha_2$	0,7386	0,7076	0,6931	0,6865	0,6831	0,6804	0,6526
α_2	42°24′	44°57	46°07′	46°39	46°55	47°07′	49°16′
$e_p = 51 - \alpha_2$	8°60	6°05	4°88	4°35	4°84	3°88	1°73

TABLE 6

i	— 15°	— 10°	— 7°30	— 5°	— 2°30	0	
$\frac{\pi}{4} - e_f$	42°24′	44°57′	46°07′	46°39′	46°55′	47°07′	
e_f	2°36′	0°03′	— 1°07′	— 1°39′	— 1°55′	— 2°07′	
$i - e_f$	— 12°24′	— 9°57′	— 8°37′	— 6°39′	— 4°25′	— 2°07′	
$\sin \psi = \sin (i - e_f)$	— 0,2148	— 0,1728	— 0,1431	— 0,1158	— 0,7701	— 0,03694	
$\cos (\psi - m)$	0,7386	0,7076	0,6931	0,6865	0,6831	0,6804	
$C_z = 2 \cdot \frac{\tau}{c_d} \cdot \frac{\sin \psi}{\cos (\psi - m)}$	0,3414	0,2806	0,2424	0,1980	0,1323	0,06373	

6.2 Evaluation of C_z

We relate the aerodynamic force to the product of the dynamic pressure /67 by the blade surface

$$C_z = \frac{\frac{q\gamma}{\tau \cdot \cos\theta_1}}{\frac{1}{2} \cdot m_s \cdot W_1^2 \cdot l \cdot c_d}$$

with

$$q = m_s \cdot W_1 \cdot l \cdot \tau \cdot \cos\theta_1,$$

$$\gamma = \frac{-\tau \cdot W_1 \cdot \sin\psi}{\cos(\psi - m)} = +\frac{\tau \cdot W_1 \cdot \sin(i - e_f)}{\cos\left(\frac{\pi}{4} + e_f\right)},$$

from which

$$C_z = -2 \cdot \frac{\tau}{c_d} \cdot \frac{\sin(i - e_f)}{\cos\left(\frac{\pi}{4} + e_f\right)}.$$

For the application considered,

$$\frac{(\tau)}{c_d} = \text{relative pitch} = 0.587 \quad \text{and} \quad \theta_1 = \frac{\pi}{4}.$$

Table 6 gives the values of C_z corresponding to this last formula. Figure 21 gives graphic representation of this and makes it possible to note that for:

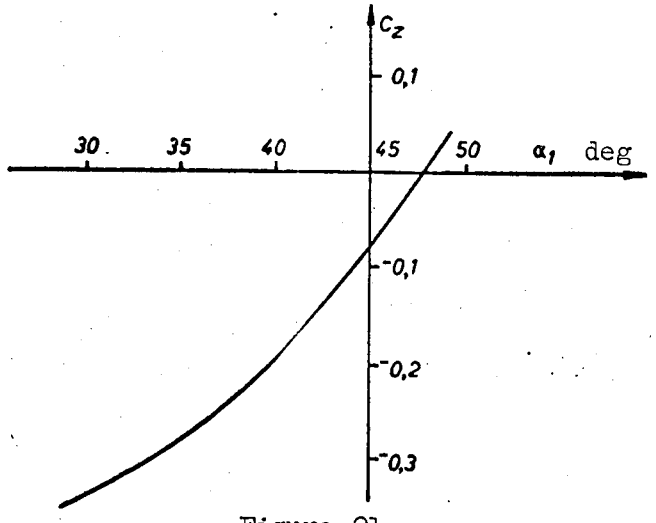

Figure 21

$i = -8^\circ\ 30'$, C_z is 0.255 theoretically and was measured as 0.240;

$i = -6^\circ\ 30'$, C_z is 0.225 theoretically and was measured as 0.200.

The difference in the two cases is less than 13 percent, i.e., low enough to confirm the theory developed in the preceding chapters.

6.3 Calculation of A_m $(W_{1,i})$

We proceed to numerical application of formula (25). /68

A. Estimated Weight of a Blade (fig. 18A)

We use 8 for the steel density and consequently

$$P = \left(1{,}7 \cdot 0.2 + \frac{\pi \cdot \frac{2}{0.2}}{8} + 1.13 \cdot 0{,}1\right) \cdot 20 \cdot 8$$
$$= (0.34 + 0.016 + 0.113) \cdot 160 = 75.04 \text{ gram}.$$

B. Expression of the Compressibility Coefficient as a Function of Velocity $W_1 = 20$ with W_{x_c} in m/sec.

$$M = \frac{W_1}{a_m\sqrt{2}}\sqrt{1 + \frac{\cos^2\left(i + \frac{\pi}{4}\right) - 0.5\sin^2 i}{\cos^2\left(\frac{\pi}{4} + e_f\right)}} \neq \frac{20}{330 \cdot \sqrt{2}}\sqrt{1 + \frac{\cos^2\left(i + \frac{\pi}{4}\right)}{\cos^2\frac{\pi}{4}}}\, W_{x_c},$$

$$M = \frac{20\, W_{x_c}}{330}\sqrt{0.5 + \cos^2\left(i + \frac{\pi}{4}\right)} = 0.0606 \cdot W_{x_c} \cdot \sqrt{0.5 + \cos^2\left(i + \frac{\pi}{4}\right)},$$

$$\sqrt{1 - M^2} \neq 1 - \frac{M^2}{2} = 1 - 0.002\, W_{x_c}^2\left\{0.5 + \cos^2\left(i + \frac{\pi}{4}\right)\right\}.$$

C. Expression of Dynamic Pressure

$$m_s \cdot (\tau) \cdot 1 \cdot W_1^2 = \frac{1.225 \cdot 10^{-3} \cdot 0.587 \cdot 20 \cdot 2.93 \cdot 4 \cdot 10^6 \cdot W_{x_c}^2}{0.981 \cdot 10^3} = 171.8\, W_{x_c}^2 \text{ g/cm}^2.$$

D. Influence of Incidence in Absence of Detachment

$$\frac{\cos^2 m \cdot \cos^2 \theta_1}{\cos^2(\psi - m)} = \frac{\cos^2\left(i + \frac{\pi}{4}\right) \cdot \cos^2 \frac{\pi}{4}}{\cos^2\left(\frac{\pi}{4} + e_f\right)} = \cos\left(i + \frac{\pi}{4}\right) \cdot \frac{0.5000}{0.6293^2} = 1.2626 \cos^2\left(i + \frac{\pi}{4}\right).$$

E. Influence of Cascade Frequency and Depth

$$\frac{\pi \cdot 981 \text{ cm/s}^2}{e\,\omega^2} = \frac{\pi \cdot 981 \cdot \sqrt{2}}{4\,\pi^2 \cdot 2{,}93 \cdot 1\,600} = 0.02355.$$

This yields in formula (25)

$$\frac{A_m - d_0}{\sin \omega\, l_d} = \frac{m_s \cdot l \cdot \tau \cdot W_1^2}{P\sqrt{1 - M^2}} \cdot \frac{\cos^2 m \cdot \cos^2 0_1}{\cos^2(\psi - m)} \cdot \frac{\pi}{e\,\omega^2},$$

$$\frac{A_m - d_0}{\sin \omega\, l_d} = \frac{171{,}8\ W_{x_c}^2 \cdot 0.02355 \cdot \cos^2\left(i + \frac{\pi}{4}\right) \cdot 1.2626}{75{,}04 \cdot (1 - 0.002) \cdot W_{x_c}^2 \cdot \left\{0{,}5 + \cos^2\left(i + \frac{\pi}{4}\right)\right\}},$$

$$\frac{A_m - d_0}{\sin \omega\, l_d} = 0.06807 \cdot \cos^2\left(i + \frac{\pi}{4}\right) \cdot \frac{W_{x_c}^2}{1 - 0.002\ W_{x_c}^2 \left\{0.5 + \cos^2\left(i + \frac{\pi}{4}\right)\right\}}.$$

F. Influence of Fluid Passage Interval Through the Cascade

$$\frac{c_d \cdot \omega}{W_m} = \omega\, l_d = \frac{2{,}93 \cdot 40 \cdot 2\,\pi}{2\,000 \cdot W_{x_c}} \cdot \frac{\sqrt{2}\cos(\psi - m)}{\sqrt{\cos^2(\psi - m) + \cos^2 m - 0.5 \sin^2 i}} \text{ rad.}$$

In conclusion, and since λ_e is a coefficient of adjustment to be determined experimentally

$$\frac{A_m}{\lambda_e} = d_0 + 0{,}06807 \cdot \cos^2\left(i + \frac{\pi}{4}\right) \cdot \frac{W_{x_c}^2}{(1 - 0.002\ W_{x_c}^2)\left\{0.5 + \cos^2\left(i + \frac{\pi}{4}\right)\right\}} \cdot \sin \Theta,$$

$$\Theta = \frac{\sqrt{2}\cos(\psi - m)}{\sqrt{\cos^2(\psi - m) + \cos^2 m - 0.5 \sin^2 i}} \cdot \frac{0.3632}{W_{x_c}}.$$

6.4 Influence of Detachment on the Damping Coefficient

This can be demonstrated by expressing the Napieran logarithm α_v of two consecutive amplitudes which is the measured magnitude, that is

$$\frac{y_{Mn}}{y_{Mn+1}} = \sqrt{\frac{\left\{e^{-(A_m/2\pi)\omega t}\left(\frac{A_m}{2\pi}-\frac{y_\infty}{y_0}\right)+\frac{y_\infty}{y_0}\right\}^2 + e^{-(A_m/\pi)\cot}}{\left\{e^{-(A_m/2\pi)\omega[t+(1/N_p)]}\cdot\left(\frac{A_m}{2\pi}-\frac{y_\infty}{y_0}\right)+\frac{y_\infty}{y_0}\right\}^2 + e^{-(A_m/2\pi)\omega[t+(1/N_p)]}}},$$

$$\frac{y_{Mn}}{y_{Mn+1}} = e^{A_m}\sqrt{\frac{\left\{\left(\frac{A_m}{2\pi}-\frac{y_\infty}{y_0}\right)+\frac{y_\infty}{y_0}e^{(A_m/2\pi)\omega t}\right\}^2+1}{\left\{\left(\frac{A_m}{2\pi}-\frac{y_\infty}{y_0}\right)+\frac{y_\infty}{y_0}e^{A_m[(\omega t/2\pi)+1]}\right\}^2+1}},$$

$$\alpha_v = A_m - \frac{1}{2}\operatorname{Log}\frac{1+\left\{\left(\frac{A_m}{2\pi}-\frac{y_\infty}{y_0}\right)+\frac{y_\infty}{y_0}\cdot e^{A_m}\cdot e^{A_m\cdot N_p t}\right\}^2}{1+\left\{\left(\frac{A_m}{2\pi}-\frac{y_\infty}{y_0}\right)+\frac{y_\infty}{y_0}\cdot e^{A_m\cdot N_p t}\right\}^2}. \tag{34}$$

The value of t, for which α_v is cancelled, is the root of the equation /70

$$e^{A_m\cdot N_p t} = \frac{e^{2A_m}-1}{2\,e^{A_m}\cdot(e^{A_m}-1)}\cdot\frac{1+\left(\frac{A_m}{2\pi}-\frac{y_\infty}{y_0}\right)^2}{\frac{y_\infty}{y_0}\cdot\left(\frac{y_\infty}{y_0}-\frac{A_m}{2\pi}\right)} \tag{35}$$

and can be specified, provided we know $\frac{y_\infty}{y_0}$ as a function of W_x, i.e., $d_p(\mathrm{Re})$.

A. However, on the hypothesis that the time elapsed between the instant of release into the wind and the instant of measurement of α_v is constant for all experiments, we can find directly the essential of the configuration of the curves $\alpha_v(W)$ shown in Recherche Aéronautique No. 71. We assume only that $\left\{\frac{d_p(\mathrm{Re})}{l\left(\frac{l}{2}\right)}\right\}$ varies little with Re and that $\frac{y_\infty}{y_0}$ is sufficiently large in relation to A_m so that we can neglect $\frac{A_m}{2\pi}$. We then have

$$e^{Am \cdot Np.\delta} \sim \frac{1}{\left(\frac{y_\infty}{y_0}\right)^2} = \frac{C^{te}}{\psi^2},$$

which gives the equation of a stability curve separating the plane W, Q into two regions

$$W = W_A - W_B \log \psi.$$

A_m is actually roughly proportional to W when Θ is sufficiently small, which is the case at velocities cancelling out α_v. Within one of these regions, damping is positive (stability), and within the other it is negative (instability). To determine this curve we use:

(1) W = 85 m/sec and $\psi = 15 + 6 = 21^\circ$, a case of cancellation of α_v actually observed at Chalais-Meudon, but not referred to in Recherche Aéronautique No. 71.

(2) W = 65 m/sec and $\psi = 17.7 + 6 = 23.7^\circ$, the case referred to in figure 11 of the Leclerc communication (R. A., No. 71); hence the numerical expression of W

$$W = \frac{1}{0.0525}(30.91 - 20 \log \psi),$$

which gives

$$W = 72 \text{ m/s} \quad \text{if} \quad \psi = 22.7^\circ;$$

These values actually correspond to the other cancellation point of α_v plotted in the same figure. Admitting that $d_p(Re)$ retains the same value although W varies, this very simple formula shows that W should exceed 120 m/sec under /71 the same experimental conditions so that α_v is cancelled when incidence drops to 10.7° (from which $\psi = 16.7^\circ$).

B. Actually, $d_p(Re)$ can have a more precise definition by classical concepts. Turbulence appears in the ducts when the Reynolds number reaches a so-called "critical" value between 1,000 and 10,000 and we formulate a probable supplementary hypothesis by using

$$\frac{d_p(Re)}{l\left(\frac{l}{2}\right)} = A_r \cdot \log \frac{Re}{10^4}$$

with

$$\mathrm{Re} = \frac{m_s \cdot W_m \cdot c_d}{\mu} \cdot \frac{\frac{l}{c_d} \cdot \frac{\tau}{c_d} \cdot \cos\theta_1}{\left\{\frac{l}{c_d} + \frac{\tau}{c_d} \cdot \cos\theta_1\right\}} = K\mu \cdot W_{x_0},$$

$$K\mu = \frac{2\, W_m\, c_d}{\nu} \cdot \frac{\frac{l}{c_d} \cdot \frac{\tau}{c_d} \cdot \cos\theta_1}{\frac{l}{c_d} + \frac{\tau}{c_d} \cdot \cos\theta_1} = \frac{4\,000 \cdot 2.93}{0.13} \cdot \frac{\frac{20}{2,93} \cdot 0.587 \cdot 0.7071}{\frac{20}{2.93} + 0.587 \cdot 0.7071},$$

$$K\mu = 9{,}016 \cdot 10^4 \cdot 0{,}3913 = 3{,}528 \cdot 10^4.$$

Determination of A_r results from formula (33) after we calculate $\frac{y_\infty}{y_0}$ on the basis of equation (35), in which we have established the difference of time elapsed between the instant of blade release into vibration and the instant of measuring the damping coefficient, that is

$$\frac{y_\infty}{y_0} = \sqrt{\frac{1}{e^{A_m \cdot N_{p.t}}}}\,. \tag{36}$$

Table 7 gives A_m for a 15° incidence for which we used an experimental adjustment coefficient from formula (25) equal to 1/6.

Finally, assuming t equal to 5 sec (a new and very probable calculation hypothesis) and by writing that the coefficient α_v is zero when the incident velocity is 85 m/sec and incidence is equal to 15°, we find

$$A_m \cdot N_{p.t} = 200 \cdot 0.01875 = 3.75,$$

$$\frac{y_\infty}{y_0} = \sqrt{\frac{1}{e^{3,75}}} = 0.1535,$$

from which

$$A_r = \frac{y_\infty}{y_0} \cdot \frac{1}{\frac{c_d\,\psi}{\cos\theta_1} \cdot \log\frac{\mathrm{Re}}{10^4}} = 0.1535 \cdot \frac{1}{\frac{2.93 \cdot 0.3665}{0.7071} \cdot \log 15}.$$

$$A_r = \frac{0.1535}{1{,}519 \cdot 1{,}176},$$

$$\frac{d_p\,(\mathrm{Re})}{l\left(\frac{l}{2}\right)} = 0.08593 \cdot \log\left\{3.528\, W_{x_0}\right\}. \tag{37}$$

It is therefore assumed that the experimental results to be compared /72
on these bases actually are comparable, i.e., that the amplitude of release into the wind $f\left(\frac{1}{2}\right)$ did not vary during the experiments and that the measurement was always carried out at the same point on the blade.

TABLE 7. EVOLUTION OF A_m IF W VARIES AND THE INCIDENCE IS -15°.

$$-\psi + m = \alpha_3 = 51°; \quad m = i + \frac{\pi}{4} = -15° + 45° = 30°; \quad \psi = -i + e_1 = 21°$$

$$\sqrt{2}\cos(\psi - m) = 1.414 \cdot 0.6293 = 0.8898; \quad 0.5 + \cos^2\left(i + \frac{\pi}{4}\right) = 1.2500$$

$$\sqrt{\cos^2(\psi - m) + \cos^2 m - 0.5\sin^2\psi} = 1.040;$$

$$0.6807 \cdot \cos^2\left(i + \frac{\pi}{4}\right) = 0.06807 \cdot 0.75 = 0.05105$$

$$\Theta = \frac{0.8898 \cdot 0.3682}{1.040 \cdot W_{x_0}} = \frac{0.3150}{W_{x_0}}; \quad \lambda_e = \frac{1}{6}$$

W_{x_0}	2	3	4	4,25
Θ	0,1575	0,1050	0,07875	0,07412
Sin Θ	0,1567	0,1048	0,07875	0,07412
$1 - 1{,}250 \cdot 0{,}002\ W_{x_0}^2$	0,9900	0,9776	0,9600	0,9548
$W_{x_0}^2$	4	9	16	18,0625
$\frac{A_m}{\lambda_e}$	0,03183	0,04878	0,06658	0,07125
A_m	0,005305	0,008130	0,01110	0,01875

C. The trace of the curve representing the variations of α_v as a function of W is then satisfactorily determined by formula (34) and was plotted in figure 22 by means of table 8. The similarity of the theoretical curve to the experimental curve is certain, specifically near the point of cancellation which served to determine the value of A_r. The relation with the experimental curves determined at the 16.7° and 17.7° incidences was investigated in A and does not call for any other comment since the general trend of the respective curves is also very similar to that of the theoretical curve.

TABLE 8. EVOLUTION OF α_v WHEN W VARIES, INCIDENCE IS -15°, AND DELAY IN MEASURING α_v IS 5 SEC.

W_{x_c}	2	3	4
$3{,}528\ W_{x_c}$	7,056	10,584	14,112
$\log \mid 3{,}528 \cdot W_{x_c} \mid$	0,84856	1,02449	1,14953
$\frac{d_p(\mathrm{Re})}{l\left(\frac{l}{2}\right)}$	0,07292	0,08799	0,09873
$\frac{c_d \cdot \mid \psi \mid}{\cos \theta_i}$	1,519	1,519	1,519
$\frac{y_\infty}{y_0}$	0,1107	0,1336	0,1500
$200\ A_m$	1,061	1,626	2,222
$e^{200 A_m}(1 + A_m)$	2,904	5,125	9,327
$\frac{y_\infty}{y_0} \mid e^{200 A_m}(1 + A_m) - 1 \mid$	0,2108	0,5512	1,249
Num. $\mid e^{200 A_m} - 1 \mid$	1,004	1,304	2,559
$\frac{y_\infty}{y_0} \mid e^{200 A_m} - 1 \mid$	0,2092	0,5458	1,234
Den. $\mid e^{-2(\alpha_v - A_m)} \mid$	1,004	1,298	2,521
$e^{-2(\alpha_v - A_m)}$	1,000	1,005	1,015
$2(\alpha_v - A_m)$	0	— 0,005	— 0,015
$\alpha_v - A_m$	0	— 0,0025	— 0,0075
α_v	0,0053	0,0056	0,0036

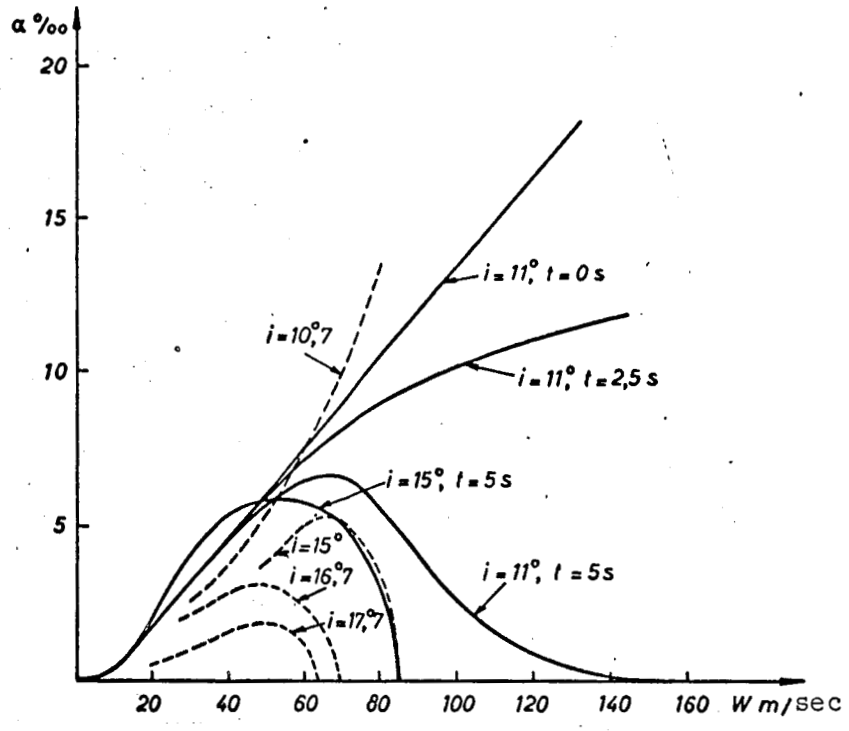

Figure 22

---, Experimental curves.

D. It remains to be shown that, at slight incidence and under the same experimental conditions, the researchers were not able to note zero values of α_v (fig. 22). /74

For this, we apply the same formula (25) for i = -11° with the same coefficient of adjustment of 1/6. Table 9 then furnishes the elements of the trace of a curve $\alpha_v(W)$ characteristic of a difference of time practically zero between the instant of release and the instant of measure. The similarity of this curve with the experimental curves determined for incidences of 10.7° and 13.7° is obvious. To take into account the delay of 5 sec in the measurement of α, we can initially determine the value of W which cancels the expression of α_v given by formula (34) if we have

$$N_{p \cdot t} = 200.$$

Equation (35)

$$\frac{1}{e^{AmNpt}} = \left(\frac{y_\infty}{y_0}\right)^2$$

TABLE 9. EVOLUTION OF A_m IF W VARIES AND THE INCIDENCE IS -11°.

$$-\psi + m = \alpha_a = 51^\circ; \qquad m = i + \frac{\pi}{4} = -11 + 45 = 34^\circ; \qquad \psi = -i + e_f = 17^\circ$$

$$\sqrt{2} \cdot \cos(\psi - m) = 1.414 \cdot 0.6293 = 0.8898; \qquad 0.5 + \cos^2\left(i + \frac{\pi}{4}\right) = 1.1872$$

$$\sqrt{\cos^2(\psi - m) + \cos^2 m - 0.5 \sin^2 \psi} = 1.019;$$

$$0.06807 \cdot \cos^2\left(i + \frac{\pi}{4}\right) = 0.06807 \cdot 0.6872 = 0.04678$$

$$\Theta = \frac{0.8898 \cdot 0.3682}{1.019 \cdot W_{x_0}} = \frac{0.3214}{W_{x_0}}; \qquad \lambda_e = \frac{1}{6}$$

W_{x_0}	2	3	4	6,5
Θ	0,1607	0,1074	0,0803	0,0493
Sin Θ	0,1599	0,1072	0,0803	0,0493
$1 - 1{,}187 \cdot 0{,}002\ W_{x_0}^2$	0,9903	0,9781	0,9606	0,8990
$W_{x_0}^2$	4	9	16	42,25
$\frac{A_m}{\lambda_e}$	0,02972	0,04564	0,06211	0,10839
A_m	0,004953	0,007607	0,01035	0,01806

or, in the case investigated earlier

$$\frac{1}{e^{200.0,01875}} = \overline{0,1535^2}$$

becomes, by linearizing the variation of A_m given in table 9 on the basis /75
of the pair ($W_x = 4$, $A_m = 0.01035$) and by taking into consideration formulas (33) and (37)

$$\frac{1}{e^{200 \cdot \frac{0.01035}{4} \cdot W_{x_0}}} = \left(0.1535 \cdot \frac{0.2967}{0.3665}\right)^2 \cdot \left(\frac{0.54753 + \log W_{x_0}}{1.176}\right)^2$$

or

$$\frac{42.5}{\left| 42.5 \right|^{0.138 W_{x_0}}} = 0.658 \left(\frac{0.5475 + \log W_{x_0}}{1,176}\right)^2.$$

TABLE 10. EVOLUTION OF α_v WHEN W VARIES, INCIDENCE IS -11° AND DELAY IN MEASURING α_v IS 5 SEC.

W_{x_0}	3	4	6,5
3,528 W_{x_c}	10,584	14,112	22,932
$\log \{ 3{,}528 \cdot W_{x_c} \}$	1,02449	1,14953	1,36040
$\frac{d_p\,(\mathrm{Re})}{f\left(\frac{l}{2}\right)}$	0,08799	0,09873	0,11690
$\frac{c_d \cdot \lvert \psi \rvert}{\cos \theta_i}$	1,229	1,229	1,229
$\frac{y_\infty}{y_0}$	0,1082	0,1214	0,1437
200 A_m	1,5214	2,0700	3,612
$e^{200 A_m}\,(1 + A_m)$	4,614	8,004	37,86
$\frac{y_\infty}{y_0} \{ e^{200 A_m}\,(1 + A_m) - 1 \}$	0,3910	0,8502	5,296
Num. $\{ e^{-2(\alpha_v - A_m)} \}$	1,1528	1,7228	29,05
$\frac{y_\infty}{y_0} \{ e^{200 A_m} - 1 \}$	0,3870	0,8406	5,200
Den. $\{ e^{-2(\alpha_v - A_m)} \}$	1,1497	1,7066	28,04
$e^{-2(\alpha_v - A_m)}$	1,002	1,0094	1,036
$2\,(\alpha_v - A_m)$	— 0,002	— 0,0094	— 0,0354
$\alpha_v - A_m$	— 0,001	— 0,0047	— 0,01770
α_v	0,0066	0,00565	0,00036

TABLE 11. EVOLUTION OF α_v WHEN W VARIES, INCIDENCE IS -11° AND DELAY IN MEASURING α_v IS 2.5 SEC.

W_{x_c}	3	4	6,5
$3{,}528\ W_{x_c}$	10,584	14,112	22,932
$\log \mid 3{,}528 \cdot W_{x_c} \mid$	1,02449	1,14953	1,36040
$\frac{d_p\,(\mathrm{Re})}{l\left(\frac{l}{2}\right)}$	0,08799	0,09873	0,11690
$\frac{c_d \mid \psi \mid}{\cos \theta_1}$	1,229	1,229	1,229
$\frac{y_\infty}{y_0}$	0,1082	0,1214	0,1437
$100\ A_m$	0,7607	1,035	1,806
$e^{100 A_m}\,(1 + A_m)$	2,157	2,843	6,196
$\frac{y_\infty}{y_0} \mid e^{100 A_m}\,(1 + A_m) - 1 \mid$	0,1252	0,2237	0,7466
Num. $\mid e^{-2(\alpha_v - A_m)} \mid$	1,016	1,050	1,557
$\frac{y_\infty}{y_0} \mid e^{100 A_m} - 1 \mid$	0,1233	0,2203	0,7309
Den. $\mid e^{-2(\alpha_v - A_m)} \mid$	1,015	1,048	1,534
$e^{-2(\alpha_v - A_m)}$	1,001	1,002	1,015
$2\,(\alpha_v - A_m)$	— 0,001	— 0,002	— 0,0149
$\alpha_v - A_m$	— 0,0005	— 0,001	— 0,00745
α_v	0,0071	0,0093	0,01141

This equation consequently admits a root in W_x between 7.3 and 7.4 and thus confirms the result announced in A. At an incidence of 11°, it would have been necessary to raise the velocity of the wind tunnel up to 150 m/sec to be able to observe zero values of α_v 5 sec after the start of the experiment. Moreover, when we use

$$N_{p.t} = 200,$$

table 10 derived from application of formula (34) on the basis of table 9 makes it possible to plot a new curve (fig. 22) which indicates an apparent residual damping of 6 °/₀₀ at 85 m/sec and an incidence of 11° 5' after the start of the experiment. /78

Table 11 shows the elements of the trace of a curve $\alpha_v(W)$ for an incidence of 11° and the observations are made only 2.5 sec after the start of the experiment and at the velocity of 85 m/sec and thus shows that the coefficient α_v continues to increase with W under these conditions.

6.5 Localization of Detachment

From the observations made at Chalais-Meudon at the velocity of 85 m/sec and reported in Recherche Aéronautique No. 71 (fig. 6, p. 61), it is possible to confirm the hypotheses made for developing formula (15) by localizing the detachments which this formula is intended to take into account numerically.

In order to follow the experimental evolution of $d_p(Re)$, we can utilize figure 23 which graphically represents the last line of table 5. Behavior during expansion without detachment from the extrados as shown in figure 18 corresponds to an effective value of m - ψ greater than 45°, that is

$$(m - \psi)_f = 45^\circ + 6^\circ = 51^\circ.$$

By designating the difference by e_p as in formula (15')

$$e_p = (m - \psi) - \left(\frac{\pi}{4} + e_f\right) = 6^\circ - e_f,$$

we obtain a function of i (or ψ) represented by figure 23 from which we can deduce $d_p(Re)$. Actually, the difference between the pseudo-amplitude of the

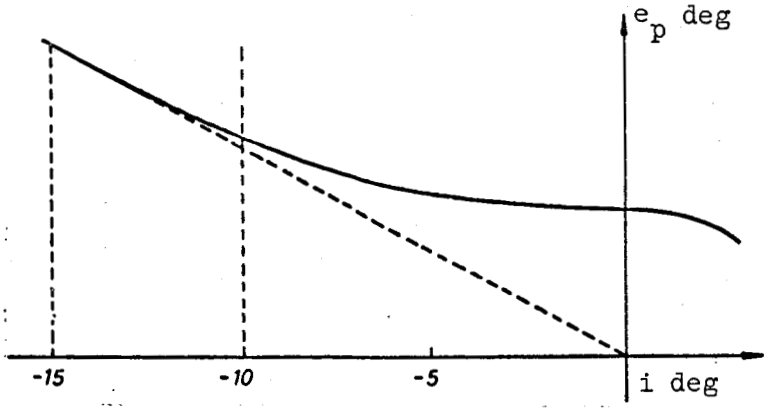

Figure 23

oscillation of the fluid and the pseudo-amplitude of the oscillation of the blade represented by $\left(\frac{d_p(\mathrm{Re})}{\cos\theta_1}\right)\cdot c_d\,.\,|\psi|$ is given by formula (15')

$$a_d\, e_p = c_d \cdot |\psi| \cdot d_p(\mathrm{Re})$$

whereas in the interval (-15° -10°) and from figure 23, we can utilize

$$e_p \text{ deg} = \frac{5.5}{10}\cdot|\psi| \text{ deg} = \frac{c_d\cdot|\psi|}{a_d}\, d_p(\mathrm{Re}),$$

from which

$$d_p(\mathrm{Re}) = \frac{5.5}{10}\cdot\frac{a_d}{c_d},$$

and finally from formulas (33) and (37)

$$\frac{5.5}{10\cdot f\left(\frac{l}{2}\right)}\cdot\frac{a_d}{c_d} = 0.08593\cdot\log|3.528\cdot 4.25|,$$

$$\frac{a_d}{f\left(\frac{l}{2}\right)} = \frac{0.8593\cdot 2.93\cdot 1.176}{5.5} \sim 0.5.$$

We see that the localized detachment responsible, in the case of vibrations at frequencies close to the natural frequency, for cancelling out aerodynamic damping takes place at a distance from the profile tip which is of the same order of magnitude as the initial amplitude at mid-height of the blade.

We now understand that the investigators:

(a) recognized on the one hand the existence on the extrados "of a detached zone of laminar regime followed by a turbulent zone slowly moving back toward the trailing edge when the incidence increases, and subsequently a detachment near the trailing edge by reason of the insufficiently progressive tip of the profile;"

(b) and considered on the other hand as valid the hypothesis of steady flow around the vibrating vanes: the oscillation of the detached zone, either on one of the faces of the profile or, at high incidence, on both sides of the tip, is localized along a band less than 1 mm wide which makes it imperceptible; its exciting effect is nevertheless sufficient to indefinitely maintain the vibrations of the blading at a very low level. It should moreover be possible to explain the "self-excited" vibrations described in reference 1 by the same process.

6.6 Phase Shift Between Blades and Influence of Relative Pitch

Since the number of vanes for the calculation step is 12, the formulation of equations (19) in Chapter 4 (Sect. 4) assumes a minimum phase shift of

$$\frac{360}{12} = 30^{\circ}$$

or a multiple of this minimum phase shift. The experimental value of 60° does not disagree with these considerations.

Failure to develop a bending flutter with the relative pitch 1.17 and 2.35, multiples of the pitch 0.587 introduced in the calculation of A_m /80

developed previously, would seem unexplainable on the other hand if it were not replaced, at high incidence, by a torsional flutter. We should remember in explanation of this phenomenon that

(a) the aerodynamic force F_y given by formula (13A) is proportional to the relative pitch, since the circulation γ is itself proportional to τ, the quotient $\frac{q}{\tau}$ itself being independent of τ;

(b) the aerodynamic force is applied at the point determined by the form of the profile and not exclusively by the velocity diagram.

It is therefore probable that, by increasing the load of the blade with the relative pitch, we increase the torsional moment to the point of converting instability due to bending flutter into an instability due to torsional

flutter. The origin of the torsional instability would be the same and could be specified by formulas analogous to those previously deduced, e.g., by the application of the second Blasius formula.

6.7 Real Frequency of Vibration

Finally, the sharp division between the bending modes (frequency of 40 cps) and the torsional mode (frequency of 663 cps) stresses the interest of investigations on the damping of vibrations in pure flexure. The fact that the vibratory frequency measured was very close to the natural frequency agrees with the preceding results, specifically those of Section 1 of Chapter 5.

REFERENCES

1. Bellenot and Lalive d'Epinay. Revue Brown Boveri, October 1950.

2. Bidard. Thermopropulsion of Planes (Thermopropulsion des avions). Gauthier-Villars, 1950.

3. Blasius. Function-theoretical Methods in Hydrodynamics (Funktionentheoretische Methoden in der Hydrodynamik). Zeitschrift für Mathematik und Physik, 1910.

4. Cisotti. Idromeccanica piana, Milan, 1922.

5. Collar. Review and Perspectives of Aeroelasticity (L'aéroélasticité, rétrospective et perspective d'avenir). Journal of the Royal Aeronautical Society, No. 577, 1959.

6. Couchet. Stresses on a Profile by an Incompressible Fluid Oscillating Around a Nonzero Incidence (Efforts d'un fluide incompressible sur un profil oscillant autour d'une incidence non nulle). ONERA, Publication No. 96, 1959.

7. Darrieus. Energy Flow in Mechanics (Le flux d'énergie en mécanique). Zeitschrift für Angewandte Mathematik und Physik, Fasc. 516, 1958.

8. Eckert. Axial and Radial Compressors (Axialkompressoren und Radialkompressoren). Berlin-Göttingen-Heidelberg, Springer, 1953.

9. Eichelbrenner. Numerical Application of a Calculation for Aerodynamic Damping of Blade Vibrations (Application numérique d'un calcul d'amortissement aérodynamique des vibrations d'aubes). ONERA, La Recherche Aéronautique, No. 46, 1954.

10. Halfmann, Johnson and Haley. Evaluation of High-Angle-of-Attack Aerodynamic Derivative Data and Stall Flutter Prediction Technique. NACA Technical Note, No. 2533, 1951.

11. Isay. Contribution to Potential Flow Through Axial Blade Cascades (Beitrag zur Potentialströmung durch axiale Schaufelgitter). Zeitschrift für Angewandte Mathematik und Mechanik, Vol. 33, 1953.

12. Giqueaux. Fluid Mechanics (Mécanique des fluides). Béranger, 1954.

13. Den Hartog. Mechanical Vibrations. McGraw Hill, 1956.

14. Haskind. Vibrations of a Cascade of Thin Profiles Under Incompressible Flow (Vibrations d'une grille de profils minces en écoulement incompressible). Journal of Applied Mathematics and Mechanics, No. 2, 1958.

15. Kampé de Fériet. Study of the Boundary Layer (Etude de la couche limite). Technique et Science aéronautiques, Vols. 4 and 5, 1943.

16. Leclerc and Legendre. Aerodynamic Damping of Bending Vibrations in a Cascade at Low Velocity (Amortissement aérodynamique des vibrations de flexion dans une grille à basse vitesse). ONERA, La Recherche Aéronautique, No. 71, 1959.

17. Legendre. On Flow in Turbines with Variable Circulation (Remarques diverses sur l'écoulement dans les turbomachines à circulation variable). ATMA, Paris, 1950.

18. --- First Elements of the Calculation of Aerodynamic Damping of Compressor Blade Vibrations (Premiers éléments d'un calcul de l'amortissement aérodynamique des vibrations d'aubes de compresseur). ONERA, La Recherche Aéronautique, No. 37, 1954.

19. --- Aerodynamic Coupling of Compressor Blade Vibrations (Couplage aérodynamique des vibrations des aubes de compresseurs). Comptes Rendus de l'Académie des Sciences, No. 10, pp. 1329-1330, 3 Sept. 1962.

20. Leray. Continuous Flow Without Friction (Ecoulements continus sans frottement). CESM, Paris, 1946.

21. Lerin. Investigation by Analogy of the Vibrations of a Compressor Cascade (Etude par analogie des vibrations d'une grille de compresseur). Note Technique ONERA, No. 8/1554 RP, 1961.

22. Lilley. An Investigation of the Flexure-torsion Flutter Characteristics of Airfoils in Cascade. The College of Aeronautics, Cranfield, Report No. 60, 1952.

23. Mazet. Mechanics of Vibration (Mécanique vibratoire). Béranger, 1955.

24. Paranjpe. Calculation of Cascade for Axial Compressors (Calcul de grille pour compresseur axial). Bulletin Escher Wyss, Vol. 3, 1960.

25. Pons. Mode of Maintaining Vibration (Mode d'entretien des vibrations). ATMA, 1935.

26. Prandtl. Wing Lift and Resistance in Theory (Trägflächenauftrieb und Widerstand in der Theorie). Jahrbuch der wissenschaftlichen Gesellschaft für Luftfahrt, 1920.

27. --- Summary of Fluid Mechanics (Précis de Mécanique des Fluides). Dunod, 1940.

28. Rainey. Preliminary Study of Some Factors Which Affect the Stall Flutter Characteristics of Thin Wings. NACA Research Memorandum L 52 D 08, July 1952.

29. Otsuka. Method of Designing Latticed Wing Profile with Prescribed Velocity Distribution. Rep. Transport, Techn. Rest. Inst., No. 16, Tokyo, 1955.

30. Schichtnig. Findings and Problems of Cascade Investigations (Ergebnisse und Probleme von Gitteruntersuchungen). Zeitschrift für Flugwissenschaften, 1953.

31. Schnittger. Vortex Flow in Axial Turbomachines. Transactions of the Royal Institute of Technology, No. 74, Stockholm, 1954.

32. Scholtz. Investigation of Flow in Blade Cascades (Strömungsuntersuchungen an Schaufelgittern). VDI Forschungsheft 442, Düsseldorf, 1954.

33. Shiori. General Theory and Stability of Pure Bending Flutter. Gov. Mach. Lab., No. 3, 1954.

34. --- Non Stall Normal Mode Flutter in Annular Cascade. Transaction of the Japan Society of Aeronautical Engineering, Vol. 1, No. 1, 1958.

35. Shirakura. Theory of Cascades Built Up of Arbitrary Blade Sections. Japan Science Review, Vol. 2, No. 3, 1952.

36. Siestrunck. Potential in Compressible Flow in Simple Helicoidal Machines (Ecoulements incompressibles à potentiel dans les machines hélicoïdales simples). ONERA, Rub. No. 32, Paris, 1949.

37. Siestrunck and Fabri. Vortical Flow in Axial Machines (Ecoulements tourbillonnaires dans les machines axiales). ONERA, Rub. No. 45, Paris, 1959.

38. Sisto. Instable Aerodynamic Reactions on Cascade Profiles (Réactions aérodynamiques instables sur des profils en cascade). Journal of Aeronautical Sciences, May 1955.

39. Söhngen. Passage of a Potential Disturbance Through a Guide-vane Ring (Durchgang einer Potentialstörung durch einen Leitschaufelkranz). Ingenieur Archiv., Vol. 20, 1952.

40. --- Aerodynamic Forces in a Vibrating Vane Ring of Small Graduation (Luftkräfte an einen schwingenden Schaufelkranz kleiner Teilung). Zeitschrift für Angewandte Mathematik und Physik, Vol. 4, 1953.

41. Speidel. Calculation of Flow Losses in Nonstaggered Plane Blade Cascades (Berechnung der Strömungsverluste von ungestaffelten ebenen Schaufelgittern). Ingenieur Archiv., Vol. 22, 1954.

42. Stanitz. Design of Two Dimensional Channels with Prescribed Velocity Distributions Along Channel Walls. NACA Report No. 1115, 1953.

43. Stodola. Steam and Gas Turbines (Turbines à vapeur et à gaz). Dunod, 1925.

44. Theodorsen. General Theory of Aerodynamic Instability of the Mechanism of Critical Vibration (Théorie générale de l'instabilité aérodynamique et du mécanisme des vibrations critiques). NACA Report No. 496, 1936.

45. Traupel. Thermal Turbines (Thermische Turbomaschinen). Springer, 1958.

46. Tsien Hshue Shen. Supersonic Flow over an Inclined Body of Revolution. Journal of Aeronautical Sciences, October 1936.

47. Villat. Fluid Mechanics (Mécanique des Fluides). Gauthier-Villars, 1930.

48. Weinig. A Generalized Method of Computing the Influence of Spacing and Stagger on the Velocity Distribution of a Profile in Cascade. Proceedings of the 4th Midwestern Conference on Fluid Mechanics, September 1955.

49. Whitehead. The Analysis of Blade Vibration Due to the Random Excitation. Aeronautical Research Council, Reports and Memoranda, No. 3253, 1962.

Translated for the National Aeronautics and Space Administration by John F. Holman and Co. Inc.